Toxicology Reports 8 (2021) 463–480

Contents lists available at ScienceDirect

Toxicology Reports

journal homepage: www.elsevier.com/locate/toxrep

Effect of embedded metal fragments on urinary metal levels and kidney biomarkers in the Sprague-Dawley rat

Jessica F. Hoffman, Vernieda B. Vergara, Anya X. Fan, John F. Kalinich *

Internal Contamination and Metal Toxicity Program, Armed Forces Radiobiology Research Institute, Uniformed Services University, Bethesda, MD, USA

ARTICLE INFO

Edited by Dr. A.M Tsatsaka

Keywords:
Embedded metals
Rat
Urine
Kidney
Biomarker

ABSTRACT

Background: Wounds with embedded metal fragments are an unfortunate consequence of armed conflicts. In many cases the exact identity of the metal(s) and their long-term health effects, especially on the kidney, are not known.

Aim of study: The aim of this study was to quantitate the urinary levels of metals solubilized from surgically implanted metal pellets and to assess the effect of these metals on the kidney using a battery of biomarker assays.

Materials and methods: Using a rodent model system developed in our Institute to simulate embedded fragment injuries, eight metals considered likely components of an embedded fragment wound were individually implanted into the gastrocnemius muscle of male Sprague-Dawley rats. The rats were followed for 12 months post-implantation with urine collected prior to surgery then at 1-, 3-, 6-, 9-, and 12-months post-implantation to provide a within-subjects cohort for examination. Urinary metal levels were determined using inductively coupled plasma-mass spectrometry and urinary biomarkers assessed using commercially available kits to determine metal-induced kidney effects.

Results: With few exceptions, most of the implanted metals rapidly solubilized and were found in the urine at significantly higher levels than in control animals as early as 1-month post-implantation. Surprisingly, many of the biomarkers measured were decreased compared to control at 1-month post-implantation before returning to normal at the later time points. However, two metals, iron and depleted uranium, showed increased levels of several markers at later time points, yet these levels also returned to normal as time progressed.

Conclusion: This study showed that metal pellets surgically implanted into the leg muscle of Sprague-Dawley rats rapidly solubilized with significant levels of the implanted metal found in the urine. Although kidney biomarker results were inconsistent, the changes observed along with the relatively low amounts of metal implanted, suggest that metal-induced renal effects need to be considered when caring for individuals with embedded metal fragment wounds.

1. Introduction

Embedded metal fragment wounds are not a new phenomenon. They have been a potential battlefield injury since the invention of gunpowder. However, because of the ballistic properties of the ammunition used in early weapons, most injuries resulted in death or traumatic amputation [1,2]. It wasn't until the development of the full metal-jacketed bullet around the time of the Spanish-American War that the survivability from battle wounds improved and the probability of embedded metal fragments increased [3]. The health risk of embedded fragments was considered low because they were considered to be inert once in the body. However, there began appearing in the scientific literature occasional individual case reports on medical issues associated with embedded fragment wounds [4–9]. In most instances, these wounds were suffered during wartime many years prior to the manifestation of the adverse health effect.

Abbreviations: AAALAC-I, Association for Assessment and Accreditation of Laboratory Animal Care International; AFRRI, Armed Forces Radiobiology Research Institute; Al, Aluminum; ALB, Albumin; ALP, Alkaline phosphatase; B2m, Beta-2-microglobulin; Co, Cobalt; Cu, Copper; DoD, Department of Defense; DU, Depleted uranium; Fe, Iron; IACUC, Institutional Animal Care and Use Committee; ICP-MS, Inductively coupled plasma-mass spectroscopy; IL-18, Interleukin-18; KIM-1, Kidney injury molecule-1; LoD, Limit of detection; LoQ, Limit of quantitation; NAG, N-acetyl-beta-D-glucosaminidase; NGAL, Neutrophil gelatinase-associated lipocalin; Ni, Nickel; OPN, Osteopontin; Pb, Lead; RBP, Retinal binding protein; Ta, Tantalum; W, Tungsten.

* Corresponding author at: 4555 South Palmer Road, Bethesda, MD, 20889, USA.
E-mail address: john.kalinich@usuhs.edu (J.F. Kalinich).

https://doi.org/10.1016/j.toxrep.2021.02.023
Received 22 December 2020; Received in revised form 20 February 2021; Accepted 23 February 2021
Available online 1 March 2021

While laboratory investigations into the health effects of embedded metals have been ongoing for many years, these studies have focused primarily on the safety of implanted medical devices [10]. Little had been done to assess the long-term health effects of military-relevant metals and metal mixtures [11]. However, that changed after the First Persian Gulf War in the early 1990′s when, as a result of friendly-fire incidents, several U.S. military personnel were wounded by depleted uranium (DU) fragments. Standard medical advice at that time was to leave embedded fragments in place. However, due to the unique chemical and radiological properties of DU, questions were raised over the wisdom of leaving these fragments in place for the life of the individual. Because of the lack of available information on the long-term effects of embedded DU, preliminary investigations into the biokinetics and toxicology of embedded DU fragments were initiated [12,13]. Furthermore, due to continuing concerns over the health and environmental effects of DU munitions, replacement materials were sought, and several tungsten-based compositions were proposed. However, when one of these compositions (tungsten/nickel/cobalt) was tested in a rodent embedded-fragment model system, it was discovered that this composition induced malignant highly-aggressive rhabdomyosarcomas at the implantation sites [14]. Conversely, a material composed of tungsten/nickel/iron did not result in any tumor formation [15,16]. These findings further underscore our dearth of knowledge with respect to the health effects of embedded fragments of military-relevant metals. Compounding the urgency of this issue is the fact that the recent conflicts in Iraq and Afghanistan have resulted in over 45,000 wounded U.S. personnel, with an estimated two-thirds of these individuals having retained metal fragments. Since standard surgical guidelines recommend leaving embedded fragments in place in an attempt to balance the potential long-term health risk of the embedded fragment with the risk of morbidity that extensive surgery brings, these wounded warriors could carry these fragments for the rest of their lives. Adding to this dilemma is that due to advances in vehicle armor and weapons design and the insurgent use of improvised explosive devices (IEDs), the list of metals and metal mixtures that may potentially be found as embedded fragments is extensive. As a result, the U.S. Department of Defense (DOD) and the Department of Veterans Affairs (DVA) have promulgated a list of “metals of concern” with respect to embedded fragments [17,18]. However, the biokinetics and toxicological properties of many of these metals when embedded as fragments are not known.

One *in vivo* property of most embedded metal fragments, regardless of the system, is that they tend to degrade over time with the resulting solubilized metal eventually excreted in the urine [12,14,19–23]. This raises a concern about both acute and chronic effects on the kidney as the solubilized metal is excreted. Although our group is focused on embedded metal fragments such as those found in shrapnel wounds, implanted medical devices have also been found to degrade and release metals *in vivo*. For example, cobalt from metal-on-metal hip replacements [24], titanium from dental implants [25], and aluminum from titanium/aluminum/vanadium joint prostheses [26] have been found in serum and urine. Previously published studies examining metal effects on kidney function focused primarily on environmental exposures, particularly through drinking water. These studies showed that a variety of non-essential metals including aluminum [27,28], nickel [29], lead [30,31], and uranium [32,33] can adversely affect kidney health. Little is known concerning the *in vivo* overload of endogenous metals on renal health, with iron being the most studied [34–36]. In addition, exposure to environmental metal pollutants via inhalation or dermal routes can also affect metal excretion patterns as well as kidney well-being [37–40]. Unfortunately, in many cases these types of exposures disproportionally affect poorer populations lacking the financial or political ability to induce change [41]. However, metals are not alone in disrupting renal health. Exposure to other toxins, including both biological and chemical, by a variety of exposure routes have been shown to induce adverse renal effects [42–45].

This work is part of a larger collaborative effort with the University of Maryland School of Medicine, the Department of Veterans' Affairs Medical Center in Baltimore, the U.S. Food and Drug Administration, and the University of Kentucky to investigate the potential health effects of embedded fragments from the “metals of concern” list in our rodent shrapnel model alongside an expanded human investigation into military personnel with a wider array of retained metal fragments. In this particular study, we followed rodents embedded with metal fragments for up to 12 months to determine urinary metal levels as a result of solubilization of the embedded fragments, as well as a series of urinary biomarkers designed to assess metal-induced renal damage.

2. Materials and methods

2.1. Animals and husbandry

All animal research in this study was approved prior to initiation by the Armed Forces Radiobiology Research Institute IACUC under protocol number 2016−05-006. All procedures involving animals were conducted in compliance with the guidelines found in the *Guide for the Care and Use of Laboratory Animals* [46] in an AAALAC-I-accredited facility. Male Sprague-Dawley (*Rattus norvegicus*) rats were utilized in these experiments and were obtained from Envigo (Barrier 208A, Frederick, MD) when approximately 30 days old and 75−100 g. After arriving at the AFRRI vivarium, rats were allowed to acclimate for at least 2 weeks prior to the start of experiments. Rats were pair-housed throughout the study in plastic microisolator cages (23.8 × 45.4 cm) with filter tops and bedding (Teklab Sani-Chips, Envigo). Bedding was changed 2–3 times per week. Animal rooms were maintained at 21 ± 2 °C with 30–70% humidity and a 12:12-h light:dark cycle (lights on at 0600). Rats were fed a standard rat chow (Teklad Global Rodent Diet 8604, Envigo) with access to water *ad libitum*.

2.2. Experimental design

Earlier work in our Institute developed a rodent model for the study of the health effects of embedded metals such as shrapnel wounds [47]. Utilizing that model, we assessed the effects of eight metals of military relevance including tungsten (W), nickel (Ni), cobalt (Co), iron (Fe), copper (Cu), aluminum (Al), lead (Pb), and depleted uranium (DU). The inert metal tantalum (Ta) was used as a control for any changes due to the surgical procedure or presence of a foreign material in the muscle. Previous work by us and others [12–14] have shown no differences between naïve rats and tantalum-implanted sham rats. As a result, the total number of animals needed for the study was reduced and the goals of the ARRIVE Guidelines met [48]. A within-subjects experimental design was used with rats (n = 8) randomly assigned to one of the nine metal implantation groups.

Metal pellets were 1 mm in diameter x 2 mm in length and were purchased from Alfa Aesar (Ward Hill, MA) with purities greater than 99.99 %, with the exception of DU pellets which were purchased from Aerojet Ordnance (Jonesboro, TN). Prior to surgical implantation, pellets were cleaned and chemically sterilized as previously described [16].

2.3. Metal implantation procedures

Metal pellets were surgically implanted into the gastrocnemius muscle of the rats as previously described [49]. Briefly, rats were initially anesthetized by administration of isoflurane (Baxter Healthcare Corp., Deerfield, IL) in an induction chamber and then maintained for the surgical period using a nose cone with a scavenger/recapture system. The surgical sites were clipped then swabbed with 70 % isopropanol followed by betadine (Purdue Pharma LP, Stamford, CT). A prophylactic dose of the analgesic buprenorphine (0.05−0.1 mg/kg, s.c., Rickitt and Colman, Hull, UK) was administered. For identification purposes, a small transponder (Electronic Lab Animal Monitoring

System, BioMedic Data Systems, Seaford, DE) was injected subcutaneously in the mid-dorsal thoracic region. The transponders were programmed with a unique animal identification number which can then be read with a low-power radio frequency scanner. An ear punch was also performed to serve as a secondary mode of identification in case of transponder failure. Using aseptic technique, an incision approximately 5 mm in length was made through the skin of each hind leg to reveal the gastrocnemius muscle. Using a 16-gauge needle and specially designed plunger, two sterile pellets were implanted into the lateral side of each gastrocnemius spaced approximately 1.5 mm apart. Following metal implantation, the incisions were sealed with tissue adhesive (VetBond, 3 M Corp, St Paul, MN). Rats were closely monitored following surgery until ambulatory. The surgical sites were examined daily for signs of inflammation, infection, and localized metal toxicity for two weeks post-surgery and then weekly thereafter for the duration of the study.

2.4. Urine collection with lab sand

Prior to pellet implantation and then at 1, 3, 6, and 9 M post-implantation, as well as immediately prior to scheduled euthanasia at 12 M post-implantation, urine samples were collected using a previously published method [50–52]. The hydrophobic sand method is less stressful than metabolic cage methods and does not introduce metal contaminants or otherwise affect urine biomarkers. Briefly, for each rat, 300-g (single pack) of hydrophobic sand (LabSand, Coastline Global, Palo Alto, CA) was spread across the bottom of a mouse plastic micro-isolation cage (15.2 cm × 25.4 cm, surface area 386 cm^2) with a filtered lid. Rats were singly placed in the prepped cage without food or water for 2 h with no further restriction on movement. Urine pooled on top of the sand and was collected immediately by pipette during each 2 h session. Samples were stored at −80 °C until analyzed.

2.5. Euthanasia and tissue collection

Upon reaching their experimental end point or when indicated by guidelines approved by the IACUC, rats were humanely euthanized by isoflurane overdose followed by exsanguination and confirmatory pneumothorax per the guidelines of the American Veterinary Medical Association [53]. Criteria for euthanasia included tumor size greater than 1 cm in diameter, loss of greater than 10 % of baseline body weight, or other indications of approaching moribundity as determined by animal health assessments. After euthanasia, a complete gross pathology examination was conducted, and a variety of tissues isolated for analysis, including brain, liver, heart, lung, popliteal lymph node, tibia, fibula, femur, gastrocnemius and triceps muscle, spleen, thymus, kidney, bladder, testes, and a fecal sample. The wet weights of liver, spleen, thymus, kidney, and testes were determined and normalized to body weight. Tissues for metal analysis were weighed and stored at −80 °C until analysis. Tissues destined for histopathology were fixed in zinc-buffered formalin and stored at 4 °C. In addition, immediately prior to euthanasia, a blood sample was collected from the abdominal aorta of the anesthetized animal to provide a sample for hematological assessment, as well as isolation of serum for clinical chemistry and metal analysis. This study focuses on results of urine sample analyses.

2.6. Metal analysis by inductively coupled plasma-mass spectroscopy (ICP-MS)

All reagents used in this study were of the highest grade available. Plastic ware and other disposables were obtained from Thermo Fisher Scientific (Pittsburgh, PA). Urine samples were diluted in ultrapure nitric acid (Optima Ultrapure Grade, Fisher Scientific, Newark, DE) and metal content determined using an inductively coupled plasma-mass spectrometer (XSeries 2 ICP-MS System, ThermoFisher, Madison, WI) equipped with a Cetac ASX520 Autosampler (Cetac Technologies, Omaha, NE). High-pressure liquid argon, 99.997 %, was used for the plasma gas. The instrument was calibrated with external standards of the appropriate metal standard (SPEX CertiPrep, Metuchen, NJ) in 2% HNO_3. The sample probe was washed with a constant flow of 2% nitric acid between measurements to prevent carryover. Quantitative analysis was obtained by reference to the slope of the calibration curve (counts per second / ng per liter) as well as an internal standard. Urine data were normalized to creatinine levels (see below). Limit of Detection (LoD)/ Limit of Quantitation (LoQ), in ppb, are as follows: Ta - 0.50/0.91; W - 0.12/0.15; Ni - 0.17/0.21; Co - 0.03/0.06; Fe - 1.08/1.85; Cu - 0.24/ 0.54; Al - 0.38/0.44; Pb - 0.02/0.04; U - 0.02/0.07.

2.7. Urine markers

2.7.1. Creatinine

Urine creatinine levels were determined by utilizing a modified Jaffe reaction [54,55] with a commercially available colorimetric kit (catalog no. CR01, Oxford Biomedical Research, Oxford, MI). Reactions were read at 490 nm in a plate reader (BioTek Synergy Model H1 M Multimodal Plate Reader with GEN5 Software, BioTek Instruments, Winooski, VT). Creatinine concentrations were determined against a standard curve (0–10.0 mg/dL) and corrected for dilution.

2.7.2. Total protein

Total protein from each urine sample was measured by Bio-Rad Protein Assay (Bio-Rad Laboratories, Hercules, CA, cat #500−0006), in triplicate, against a BSA standard curve, in a plate reader (BioTek Synergy) at 595 nm.

2.7.3. Alkaline phosphatase

Urinary alkaline phosphatase levels were determined using a colorimetric kit (kit # ab83369, Abcam, Cambridge, MA). The kit uses p-nitrophenyl phosphate (pNPP) as a phosphatase substrate which turns yellow when dephosphorylated by alkaline phosphatase. Briefly, samples and pNPP are added to a 96-well plate and incubated at room temperature for 60 min. After adding stop solution, the plate is read at 405 nm in a spectrophotometer (BioTek Synergy). Alkaline phosphate concentration is read from a standard curve and expressed as μmol/min/mL or μU/mL with an assay range of 10–250 μU.

2.7.4. Beta-2-microglobulin

Urinary beta-2-microglobulin (B2m) was measured using an ELISA kit (kit # 80666, Crystal Chem Inc., Elk Grove Village, IL). The kit uses a double antibody sandwich technique where the B2m in the sample binds to antibodies against B2m bound to the surface of a 96-well plate. Use of a second anti-B2m antibody conjugated to horseradish peroxidase (HRP) allows for the determination of beta-2-microglobulin levels against a standard curve. Briefly, diluted samples are added to the antibody-coated plate and incubated at room temperature for 60 min. After washing, the B2m antibody-HRP conjugate is added and the plate incubated in the dark at room temperature for 10 min. After washing the plate, HRP Substrate Solution, contained in the kit, is added and the plate incubated in the dark at room temperature for 10 min. After stopping the reaction, the plate is read at both 450 and 630 nm in a plate reader (BioTek Synergy). After subtracting the 630 nm reading from the 450 nm reading to correct for background, the amount of B2m in the sample can be determined from a standard curve as ng/mL, with an assay range of 0.156–5 ng/ml.

2.7.5. N-Acetyl-beta-D-glucosaminidase

N-Acetyl-beta-D-glucosaminidase (NAG) urinary levels were determined using a colorimetric kit (kit # 80390, Crystal Chem Inc.) based on the ability of NAG to hydrolyze 2-methoxy-4-(2′-nitrovinyl)-phenyl-2-acetoamido-2-deoxy-β-D-glucopyranoside to 2-methoxy-4-(2′-nitrovinyl)-phenol. Making the reaction mixture alkaline results in color development of the product that can be detected at 505 nm. Briefly, the assay involves mixing two of the kit reagents and adding that to diluted

urine samples in a 96-well plate. The plate is then incubated at 37 °C on a plate shaker (VWR International, Radnor, PA) at 200 rpm for 5 min. After an initial absorbance reading at 505 nm in a plate reader (BioTek Synergy), alkaline color development reagent from the kit is added and the plate incubated for 1 min at 37 °C and 200 rpm on a plate shaker before a second absorbance reading at 505 nm. Subtracting the initial reading from the second reading at 505 nm gives the change in absorbance per min. This result is compared to the calibration standard supplied in the kit to obtain NAG concentration in the sample expressed as IU/L. The linear assay range of the procedure is 0–200 IU/L.

2.7.6. Retinol binding protein

Urinary levels of retinol binding protein (RBP) were determined using a sandwich ELISA method (kit # ab203362, Abcam). Briefly, diluted urine samples and the Antibody Cocktail mixture, consisting of anti-RBP antibody and HRP-conjugated detection antibody, provided in the kit are added to an antibody-coated plate and incubated for 1 h at room temperature on a plate shaker (VWR International) set at 400 rpm. After extensive washing, the HRP substrate 3, 3′, 5, 5′-tetramethylbenzidine (TMB) is added and the plate incubated with shaking (400 rpm) for 10 min in the dark at room temperature to allow for color development. After stopping the reaction, the plate is read at 450 nm in a plate reader (BioTek Synergy). The amount of RBP in the sample is determined using a standard curve and is expressed as pg/mL. The reported assay linear range is 13.3–850 pg/ml.

2.7.7. Interleukin-18

Interleukin-18 (IL-18) levels in the collected rat urine were assessed using a sandwich ELISA (kit # EKF57851, Biomatik, Wilmington, DE). Briefly, after an initial plate washing, samples and standards are added and the plate incubated at 37 °C for 90 min on a plate shaker (VWR International) set at 200 rpm. After washing, biotin-labeled antibody is added, and the plate incubated at 37 °C for 60 min on a plate shaker set at 200 rpm. After extensive washing, HRP-streptavidin conjugate is added to the plate and again incubated at 37 °C and 200 rpm; this time for 30 min. After additional washes, TMB substrate is added and the plate incubated at 37 °C and 200 rpm, in the dark, for up to 30 min. After the addition of Stop Solution, the plate is read at 450 nm in a plate reader (BioTek Synergy). The amount of IL-18 present is determined from a standard curve. Reported linear range of the assay is 31.25–2000 pg/ml.

2.7.8. Kidney Injury Molecule-1, neutrophil gelatinase-associated lipocalin, albumin, and osteopontin

Urinary levels of Kidney Injury Molecule-1 (KIM-1), neutrophil gelatinase-associated lipocalin (NGAL), albumin, and osteopontin (OPN) were determined using the rat kidney injury panel 1 kit from Meso Scale Discovery (kit # K15162C, Rockville, MD). The technique uses a special electrode-containing 96-well plate coated with the appropriate capture antibodies to bind the analytes of interest. Addition of detection antibodies conjugated to a proprietary chemiluminescence tag allow quantitation of the targeted proteins using a Meso Scale Discovery QuickPlex Reader. The instrument applies a voltage to the electrodes in the plate that causes the tagged detection antibodies to emit light. The intensity of the light provides a quantitative measure of the analytes in the urine sample, with concentrations determined by comparison to a standard curve. Reported linear ranges of the procedure are as follows: KIM-1 (0.135–9.86 ng/ml); NGAL (0.316–230 ng/ml); albumin (67.2–49000 ng/ml); and OPN (0.0711–51.8 ng/ml).

2.8. Histopathology

Tissues for histopathology were fixed in zinc-buffered formalin (Z-Fix; Anatech Ltd, Battle Creek, MI), processed and embedded in paraffin, sectioned at 5–6 mm, and stained with hematoxylin and eosin. Histopathological assessments were conducted by a board-certified veterinary pathologist.

Table 1
ICP-MS Operating Conditions and Parameters.

Instrument Parameters	
Nebulizer type	Concentric
Spray chamber	Conical, with impact bead
Sampler cone	Platinum, 1 mm orifice diameter
Skimmer cone	Platinum, 0.7 mm orifice diameter
Sample uptake rate	1.0 mL/min
Sample read delay	45 s
Plasma conditions	
RF power	1400 W
Plasma argon gas flow	13.0 L/min
Auxiliary argon gas flow	0.80 L/min
Nebulizer gas flow	0.91 L/min
Mass spectrometer settings	
Scanning mode	Peak jump
Sweeps	100
Dwell time	500 μs
Channels/mass	1
Acquisition time	10 s
Number of readings/replicate	3
Number of replicates	2

2.9. Statistical analysis

The 12 M-implant group had urine collected at every time point (pre-surgery (PS), 1 M, 3 M, 6 M, 9 M, and 12 M) using LabSand, and thus metal and biomarker analysis using these samples were analyzed as within-subjects repeated measures (across time): two-way ANOVA, with Sidak's multiple comparisons test post-hoc. Mixed-model analysis is used instead of ANOVA if data is missing. Analyses were performed using GraphPad Prism Software (version 8.0.1, La Jolla, CA). In all cases P values < 0.05 were considered significant.

3. Results

In this study, male Sprague-Dawley rats were surgically implanted in the gastrocnemius muscle with pellets of military-relevant metals (2 pellets per leg). Using the LabSand technique, urine was collected prior to surgery, then at 1 M, 3 M, 6 M, 9 M, and 12 M post-implantation to provide urine for a within-subjects evaluation of metal excretion and urinary biomarkers.

3.1. Urinary metals

Operating conditions and parameters for the ICP-MS are found in Table 1. Urine metal concentrations, normalized to creatinine levels, are presented in Fig. 1. Tungsten values are presented in Panel A, comparing Ta-implanted (control) rats to W-implanted rats; $F_{time}(560) = 45.27$, $p < 0.0001$, $F_{metal}(114) = 156.4$, $p < 0.0001$, $F_{interaction}(560) = 20.37$. At all times from implant with the exception of pre-surgery (PS), W was higher in urine from the W-implanted animals than from Ta-implanted animals (1 M, 3 M, 6 M, 9 M, 12 M, *$p < 0.0001$ for all). Nickel values are presented in Panel B, comparing Ta-implanted rats to Ni-implanted rats; $F_{time}(332) = 33.47$, $p < 0.0001$, $F_{metal}(114) = 124.8$, $p < 0.0001$, $F_{interaction}(332) = 30.14$, $p < 0.0001$, noting that analysis drops the 9 M and 12 M groups because Ni-animals were euthanized prior to this point due to tumor formation and no data exists for comparison. Ni was higher in urine from the Ni-implanted animals compared to the Ta-implanted animals at 1 M, 3 M, and 6 M collection times (*$p < 0.0001$ for all). Cobalt values are presented in Panel C, comparing Ta-implanted rats to Co-implanted rats; $F_{time}(557) = 5.032$, $p = 0.0007$, $F_{metal}(114) = 54.67$, $p < 0.0001$, $F_{interaction}(557) = 4.760$, $p = 0.0011$. Co was higher in urine from the Co-implanted rats than from Ta-implanted rats at all

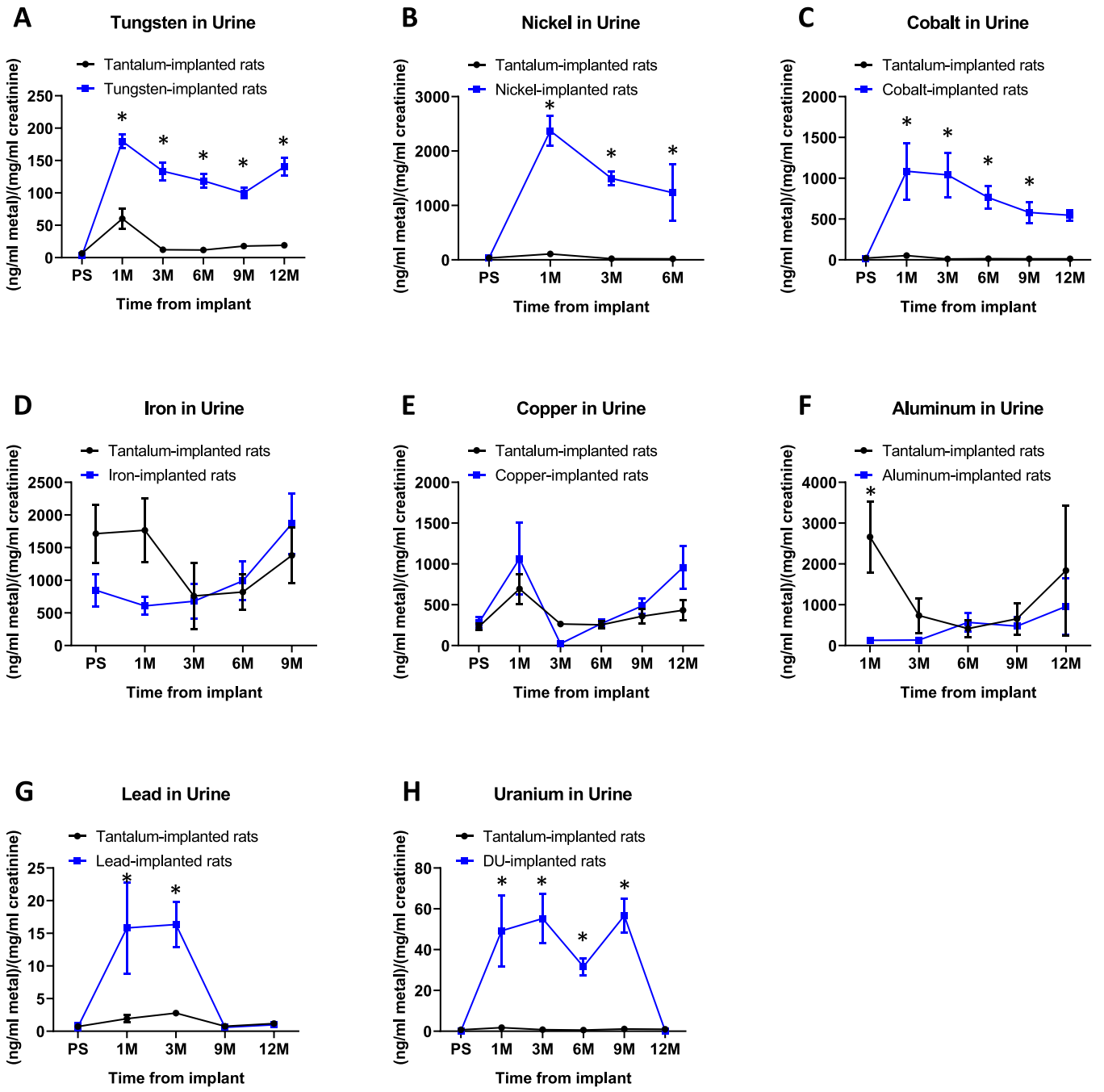

Fig. 1. Urinary metal concentrations.
Data presented as target metal concentration normalized to creatinine values in urine collected from multiple time points from individual animals. Each panel compares values in urine from the Ta-implanted animals as controls (black circles/line) vs specific target metal-implanted animals (blue squares/line). (A) tungsten, (B) nickel, (C) cobalt, (D) iron, (E) copper, (F) aluminum, (G) lead, (H) uranium. Error bars represent standard error of the mean. An * indicates a post-hoc test between Ta- and target metal-animals at that time point, $p < 0.05$.

collection times except PS and 12 M (1 M and 3 M *$p < 0.0001$, 6 M *$p = 0.0005$, 9 M *$p = 0.0094$). Iron values are presented in Panel D, comparing Ta-implanted rats to Fe-implanted rats; $F_{time}(442) = 1.662$, $p = 0.1769$, $F_{metal}(114) = 1.248$, $p = 0.2828$, $F_{interaction}(442) = 2.327$, $p = 0.0718$, noting that the 12 M data set was dropped from analysis due to lack of adequate urine samples. There were no significant post-hoc differences between metal and control at any time period.

Copper values are presented in Panel E, comparing Ta-implanted rats to Cu-implanted rats; $F_{time}(555) = 6.143$, $p = 0.0001$, $F_{metal}(114) = 1.393$, $p = 0.2576$, $F_{interaction}(555) = 1.264$, $p = 0.2927$. There were no significant post-hoc differences between metal and control at any time period. Aluminum values are presented in Panel F, comparing Ta-implanted rats to Al-implanted rats; $F_{time}(442) = 1.848$, $p = 0.1377$, $F_{metal}(114) = 4.076$, $p = 0.0631$, $F_{interaction}(442) = 2.876$, $p = 0.0342$, noting the PS data set was dropped from analysis due to errors measuring Al for this set. Aluminum in urine from the control Ta-implanted animals is higher than in Al-implanted animals at 1 M (*$p = 0.0023$) but is not significantly different at any other time point. Lead values are presented in Panel G, comparing Ta-implanted rats to Pb-implanted rats; $F_{time}(452) = 6.829$, $p = 0.0002$, $F_{metal}(114) = 10.71$, $p = 0.0019$, $F_{interaction}(452) = 4.554$, $p = 0.0031$, noting the 6 M data set was dropped from analysis due to lack of adequate urine samples. Pb

Table 2
Potential Urinary Biomarkers of Kidney Injury.

Nephron Location	Marker(s)
Glomerulus	Albumin, β2m
Proximal Tubule	Albumin, β2 m, IL-18, KIM-1, NGAL, NAG, OPN, RBP
Loop of Henle	OPN
Distal Tubules	OPN, NGAL, NAG, IL-18, ALP
Collecting Duct	NGAL

was higher in urine from Pb-implanted animals compared to Ta-implanted animals at 1 M (*p = 0.0016) and 3 M (*p = 0.0008) after implant. Uranium values are presented in Panel H, comparing Ta-implanted rats to DU-implanted rats; $F_{time}(553) = 8.153$, $p < 0.0001$, $F_{metal}(114) = 40.49$, $p < 0.0001$, $F_{interaction}(553) = 7.881$, $p < 0.0001$. Uranium was higher in urine from DU-implanted animals compared to Ta-implanted animals for all time points except pre-surgery (PS) and 12 M (1 M, 3 M, and 9 M *<0.0001, 6 M *p = 0.0028).

3.2. Urinary biomarkers

An overview of urinary markers associated with the site of potential nephron damage is given in Table 2. As can be seen, most nephron locations are represented by multiple markers and markers can be linked to more than one location. The compiled urinary marker data is

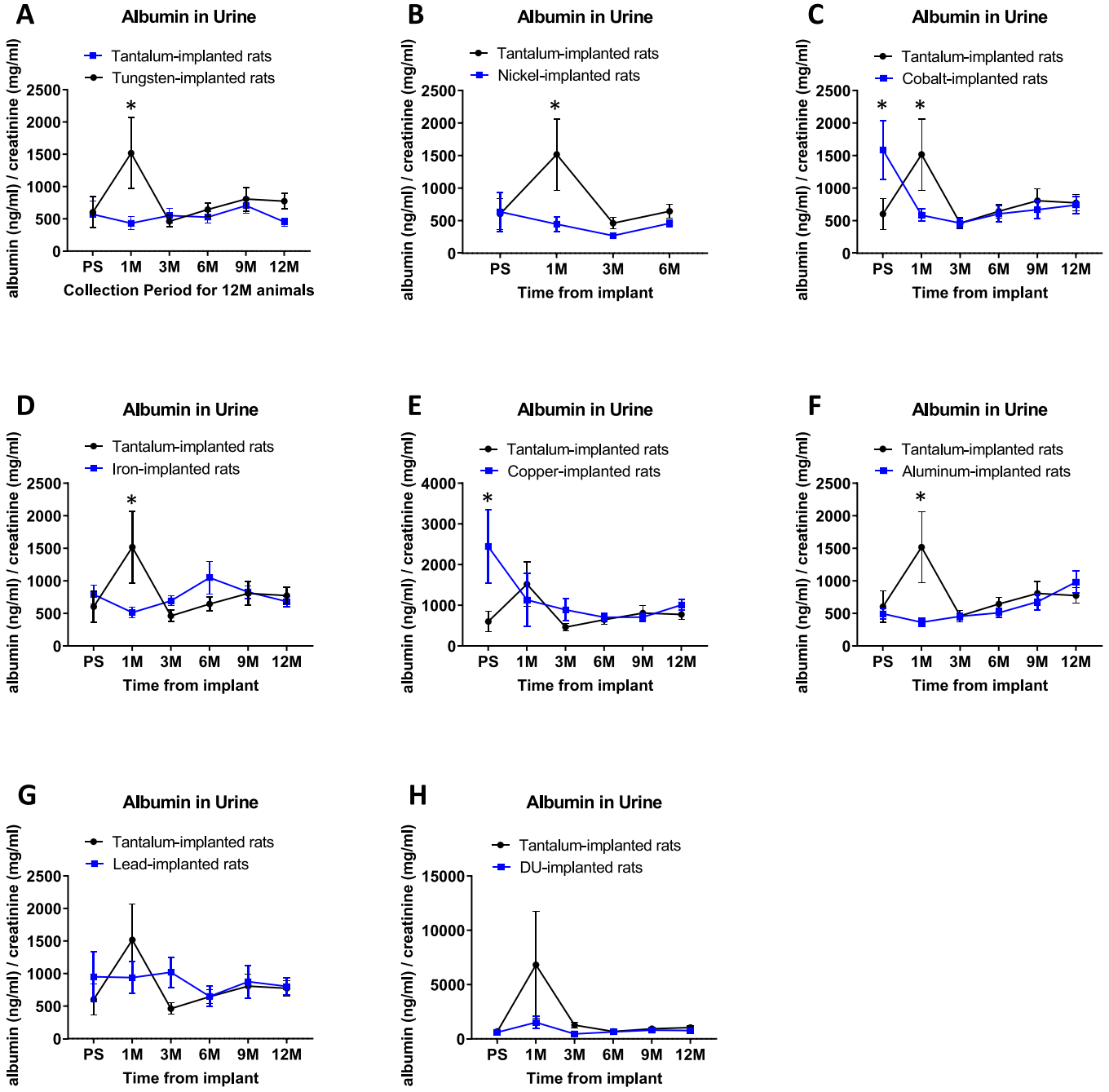

Fig. 2. Urinary albumin levels.
Data presented as albumin normalized to creatinine values in urine collected from multiple time points from individual animals. Each panel compares values in urine from the Ta-implanted animals as controls (black circles/line) vs specific target metal-implanted animals (blue squares/line). Error bars represent standard error of the mean. An * indicates a significant difference between Ta- and target metal-animals at that time point, $p < 0.05$.

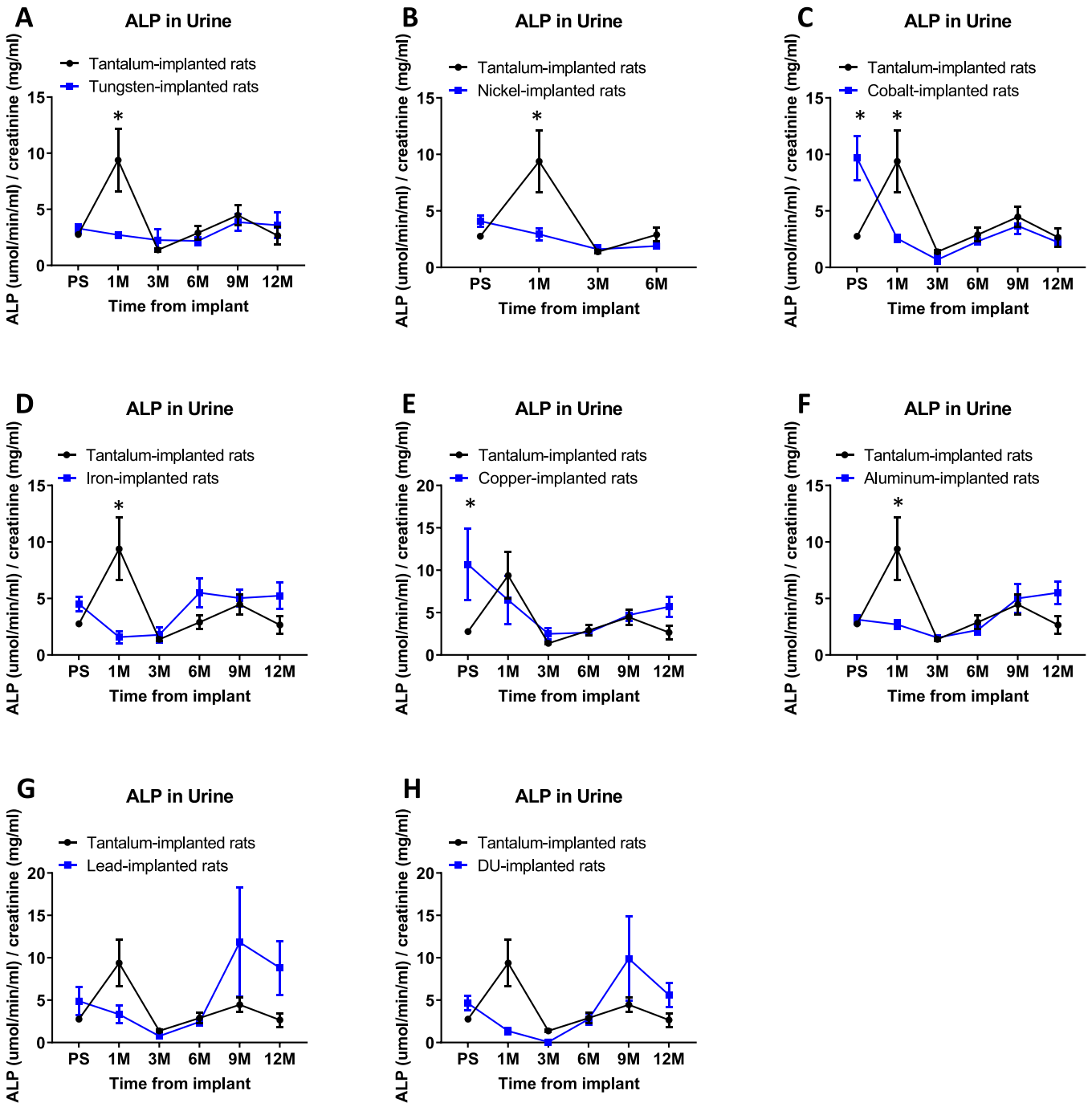

Fig. 3. Urinary ALP levels.
Data presented as ALP normalized to creatinine values in urine collected from multiple time points from individual animals. Each panel compares values in urine from the Ta-implanted animals as controls (black circles/line) vs specific target metal-implanted animals (blue squares/line). Error bars represent standard error of the mean. An * indicates a significant difference between Ta- and target metal-animals at that time point, $p < 0.05$.

presented as a figure for each individual urinary marker. Within each figure, data is always presented as the black circles/line as the values for the Ta-implanted (control) animals, and the blue squares/line as the values for the test metal-implanted animals. Panels follow the pattern of (A) tungsten, (B) nickel, (C) cobalt, (D) iron, (E) copper, (F) aluminum, (G) lead, and (H) DU. F-value statistics for the metal, time from implant, and interaction variables are listed in the figure legend. Just like with metal analysis, all biomarker analyses in panel B (Ta-implanted vs Ni-implanted) drop the 9 M and 12 M groups because Ni-animals were euthanized prior to this point due to tumor formation at the pellet implantation site and therefore no data exists for comparison. In addition, assay values for IL-18 were below the limit of detection (data not shown).

Albumin values are presented in Fig. 2. In the pre-surgery urine collection, even though no embedded metal is present, albumin is higher in urine from Co-implanted animals (*$p = 0.0128$) and Cu-implanted animals (*$p = 0.0277$) than Ta-implanted animals. At the 1 M collection time point, albumin is lower in urine from W-, Ni-, Co-, Fe-, Cu-, and Al-implanted animals than from Ta-implanted animals (*$p = 0.0006$, *$p = 0.0041$, *$p = 0.0301$, *$p = 0.0038$, and 1 M *$p = 0.0002$, respectively). There were no other significant differences in urine albumin concentration between Ta- and other metal-implanted animals.

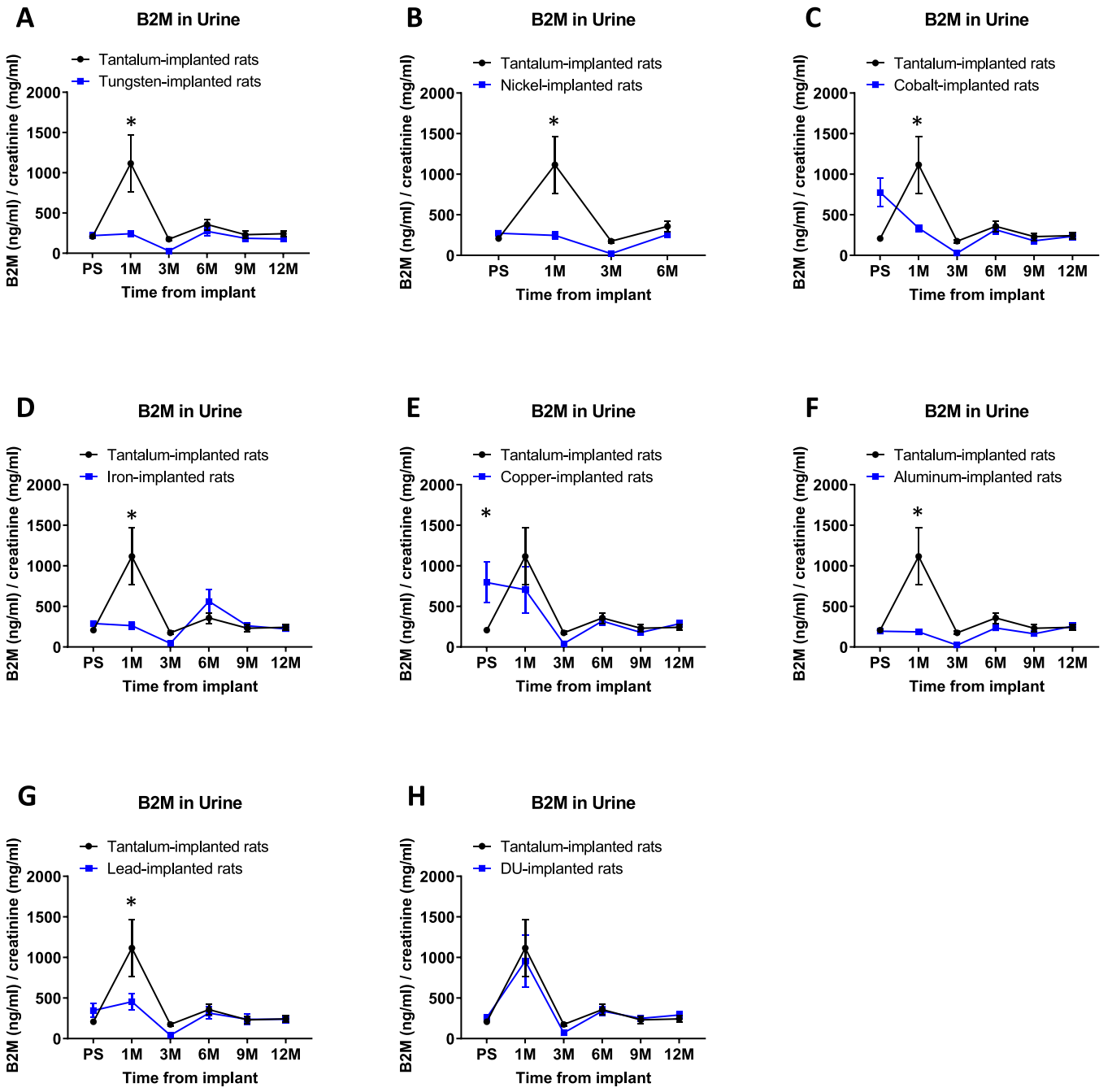

Fig. 4. Urinary B2m levels.
Data presented as B2m normalized to creatinine values in urine collected from multiple time points from individual animals. Each panel compares values in urine from the Ta-implanted animals as controls (black circles/line) vs specific target metal-implanted animals (blue squares/line). Error bars represent standard error of the mean. An * indicates a significant difference between Ta- and target metal-animals at that time point, $p < 0.05$.

ALP values are presented in Fig. 3. Similar to albumin, ALP is higher in urine from Co-implanted animals (*$p < 0.0001$) and Cu-implanted animals (*$p = 0.0002$) than from Ta-implanted animals at the pre-surgery collection period. At the 1 M collection time point, ALP is lower in urine from W-, Ni-, Co-, Fe-, and Al-implanted animals than from Ta-implanted animals (*$p < 0.0001$, *$p = 0.0002$, *$p = 0.0003$, *$p < 0.0001$, and *$p < 0.0001$, respectively). There were no other significant differences in urine ALP concentration between Ta- and other metal-implanted animals.

B2m values are presented in Fig. 4. In the pre-surgery collection period B2m is higher in urine from Cu-implanted animals than from Ta-implanted animals (*$p = 0.0415$). In the 1 M collection time point B2m is lower in urine from W-, Ni-, Co-, Fe-, and Al-implanted animals than from Ta-implanted animals (*$p < 0.0001$, *$p < 0.0001$, *$p < 0.0001$, *$p < 0.0001$, *$p < 0.0001$, and *$p = 0.0011$, respectively). There were no other significant differences in urine B2m concentration between Ta- and other metal-implanted animals.

NAG values are presented in Fig. 5. In the 1 M collection time point NAG is lower in urine from Ni-implanted animals than from Ta-implanted animals (*$p = 0.0015$). At the 9 M collection time point, NAG is lower in urine from Co- and Cu-implanted animals than from Ta-implanted animals (*$p < 0.0001$ and *$p = 0.0436$, respectively), but higher in DU-implanted animals compared to Ta-implanted controls (*$p < 0.0001$). There were no other significant differences in urine NAG

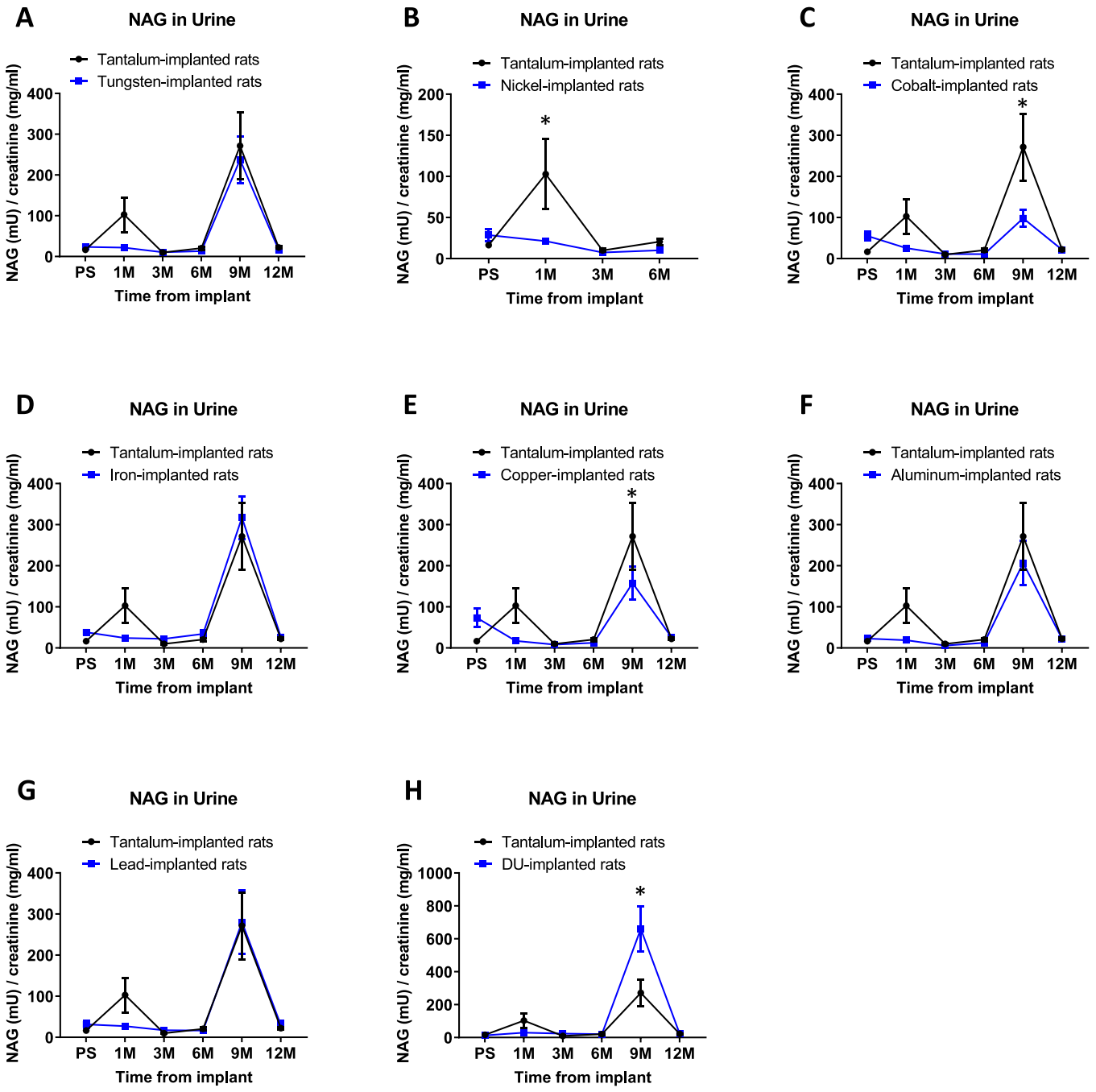

Fig. 5. Urinary NAG levels.
Data presented as NAG normalized to creatinine values in urine collected from multiple time points from individual animals. Each panel compares values in urine from the Ta-implanted animals as controls (black circles/line) vs specific target metal-implanted animals (blue squares/line). Error bars represent standard error of the mean. An * indicates a significant difference between Ta- and target metal-animals at that time point, $p < 0.05$.

concentration between Ta- and other metal-implanted animals.

RBP values are presented in Fig. 6. RBP is higher in urine from W-implanted animals than Ta-implanted animals at the 9 M time point (*$p < 0.0001$), higher in urine from Fe-implanted animals than Ta-implanted animals at the 6 M time point (*$p = 0.0308$), and higher in urine from DU-implanted animals than Ta-implanted animals at the 3 M time point (*$p = 0.0193$). There were no other significant differences in urine RBP concentration between Ta- and other metal-implanted animals.

NGAL values are presented in Fig. 7. In the pre-surgery urine collection, even though no embedded metal is present, NGAL is higher in urine from Co-implanted animals (*$p = 0.0182$) and Cu-implanted animals (*$p = 0.0024$) than Ta-implanted animals. At the 1 M collection time point, albumin is lower in urine from W-, Ni-, Co-, Fe-, and Al-implanted animals than from Ta-implanted animals (*$p < 0.0001$, *$p = 0.0003$, *$p = 0.0083$, *$p = 0.0101$, and *$p < 0.0001$, respectively). At the 6 M collection time point, NGAL is higher in urine from Fe-implanted animals than from Ta-implanted animals (*$p = 0.0003$). There were no other significant differences in urine NGAL concentration between Ta- and other metal-implanted animals.

OPN values are presented in Fig. 8. The only significant difference in OPN expression was at the 3 M collection time point, OPN is higher in urine from DU-implanted animals than Ta-implanted animals (*$p = 0.0003$).

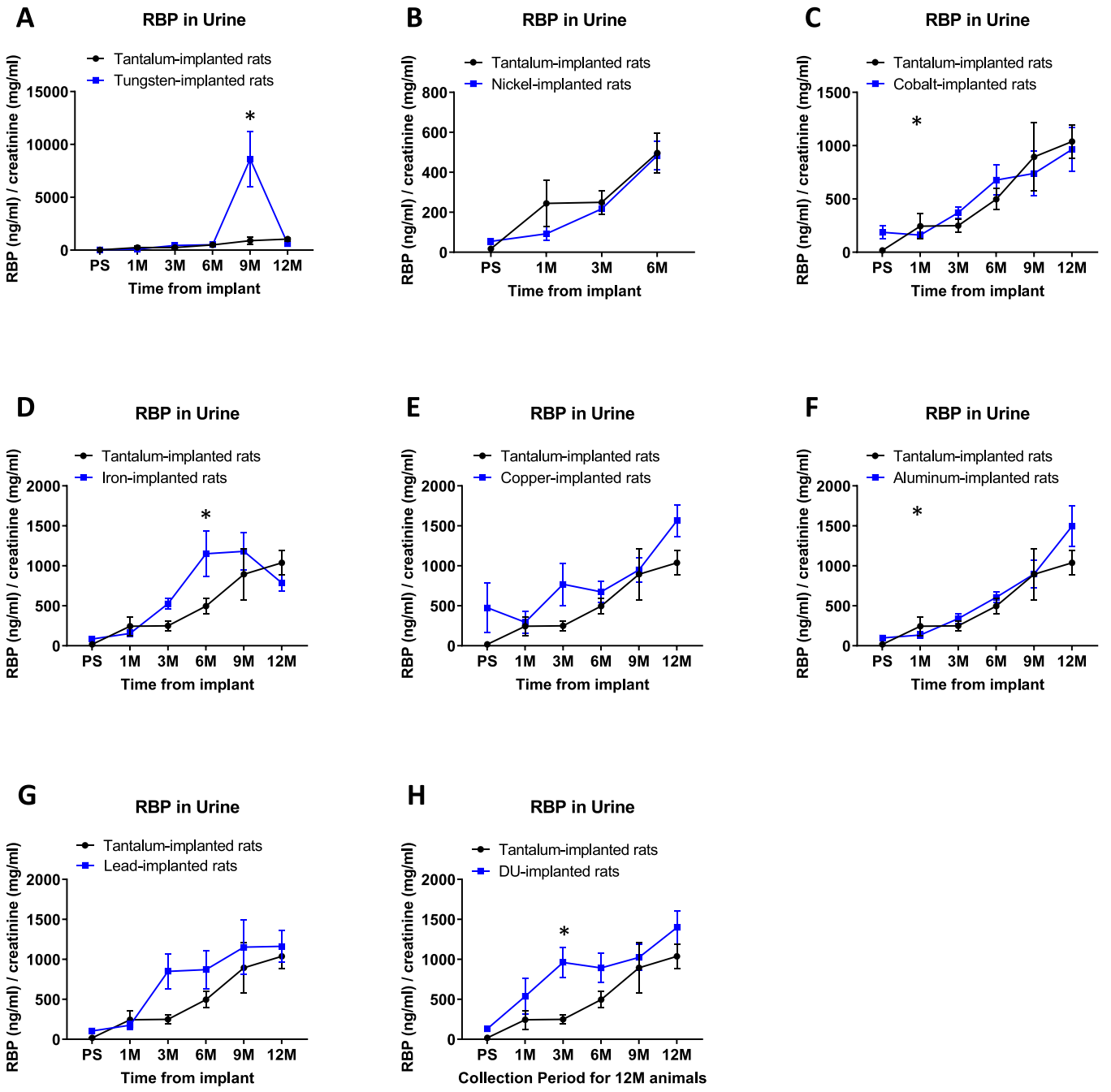

Fig. 6. Urinary RBP levels.
Data presented as RBP normalized to creatinine values in urine collected from multiple time points from individual animals. Each panel compares values in urine from the Ta-implanted animals as controls (black circles/line) vs specific target metal-implanted animals (blue squares/line). Error bars represent standard error of the mean. An * indicates a significant difference between Ta- and target metal-animals at that time point, $p < 0.05$.

KIM-1 values are presented in Fig. 9. In the pre-surgery urine collection KIM-1 is higher in urine from Co-, Cu-, and Al- implanted animals than Ta-implanted animals (*p = 0.0009, *p = 0.0018, and *p = 0.0189, respectively). At the 1 M collection time point, KIM-1 is lower in urine from W- and Ni-implanted animals than from Ta-implanted animals (*p = 0.0049 and *p = 0.0003). KIM-1 is higher in urine from Fe-implanted animals than Ta-implanted animals at the 6 M collection time point (*p = 0.0011).

Total protein values are presented in Fig. 10. In the pre-surgery urine collection total protein is higher in urine from Co- and Cu- implanted animals than Ta-implanted animals (*p = 0.0071 and *p = 0.0153, respectively), and at the 1 M urine collection time point total protein is lower in urine from W- and Ni-implanted animals compared to urine from Ta-implanted animals (*p = 0.0463 and *p = 0.0041, respectively).

Creatinine values are used to normalize other urine biomarker values because it is a commonly accepted value to correct for changes in urine volumes, especially in spot tests like the collections with LabSand. Raw values of creatinine collected from all urines are shown in Fig. 11. There is some variation within animals across time as well as between implant treatment groups. Two points of note is that the creatinine in urine from the Ta-implanted 1 M time from implant collection period is the lowest of all the Ta-implanted animal urines, as well as the lowest of all of the urines collected during this time period. This could explain why so many

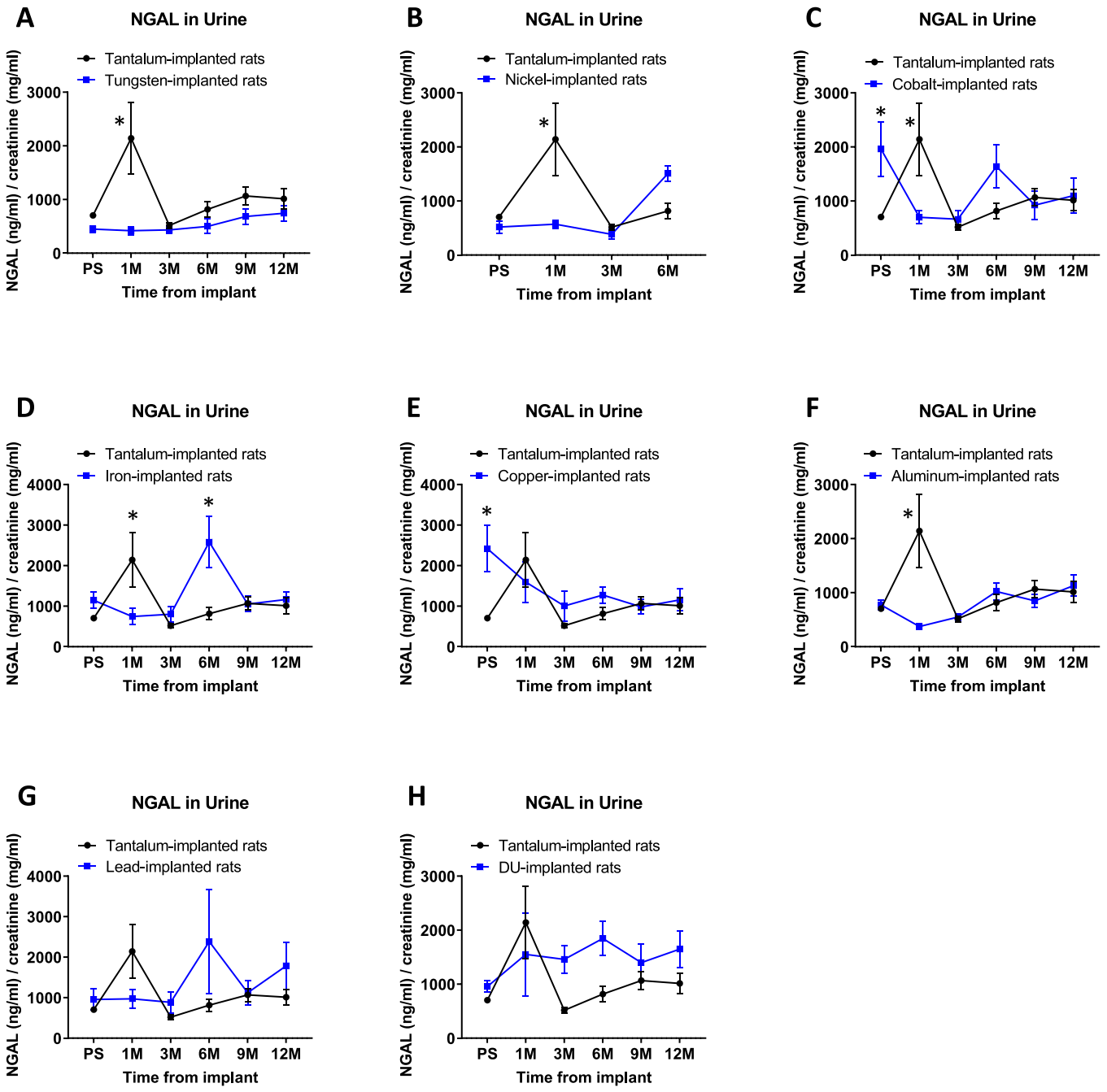

Fig. 7. Urinary NGAL levels.
Data presented as NGAL normalized to creatinine values in urine collected from multiple time points from individual animals. Each panel compares values in urine from the Ta-implanted animals as controls (black circles/line) vs specific target metal-implanted animals (blue squares/line). Error bars represent standard error of the mean. An * indicates a significant difference between Ta- and target metal-animals at that time point, $p < 0.05$.

biomarkers are higher in the Ta-implanted animals compared to the other metal-implanted animals at the 1 M time point. Similarly, the Ni-implanted animals had a very high level of creatinine compared to all the other groups at the 3 M time period.

To examine the overall variation in the urinary biomarkers, a "heat map" depicting biomarker changes is displayed in Fig. 12. Significant decreases (red squares) are seen in many of the biomarkers at the 1 M post-implantation time point for several of the metals most notably W, Ni, Co. Fe, and Al. These markers were then not statistically different than control values (yellow squares) at subsequent assay points. Both Fe- and DU-implanted rats showed significantly increased excretion of several biomarkers over control (green squares) at later time points, although this increase was transient. However, the biomarkers that were increased are indicative of proximal tubule damage.

3.3. Histopathology

Histopathological examination of kidneys from the metal-implanted rats showed no metal-specific abnormalities. Chronic progressive nephropathy was observed in all experimental groups; however, this is a common age- and strain-related condition.

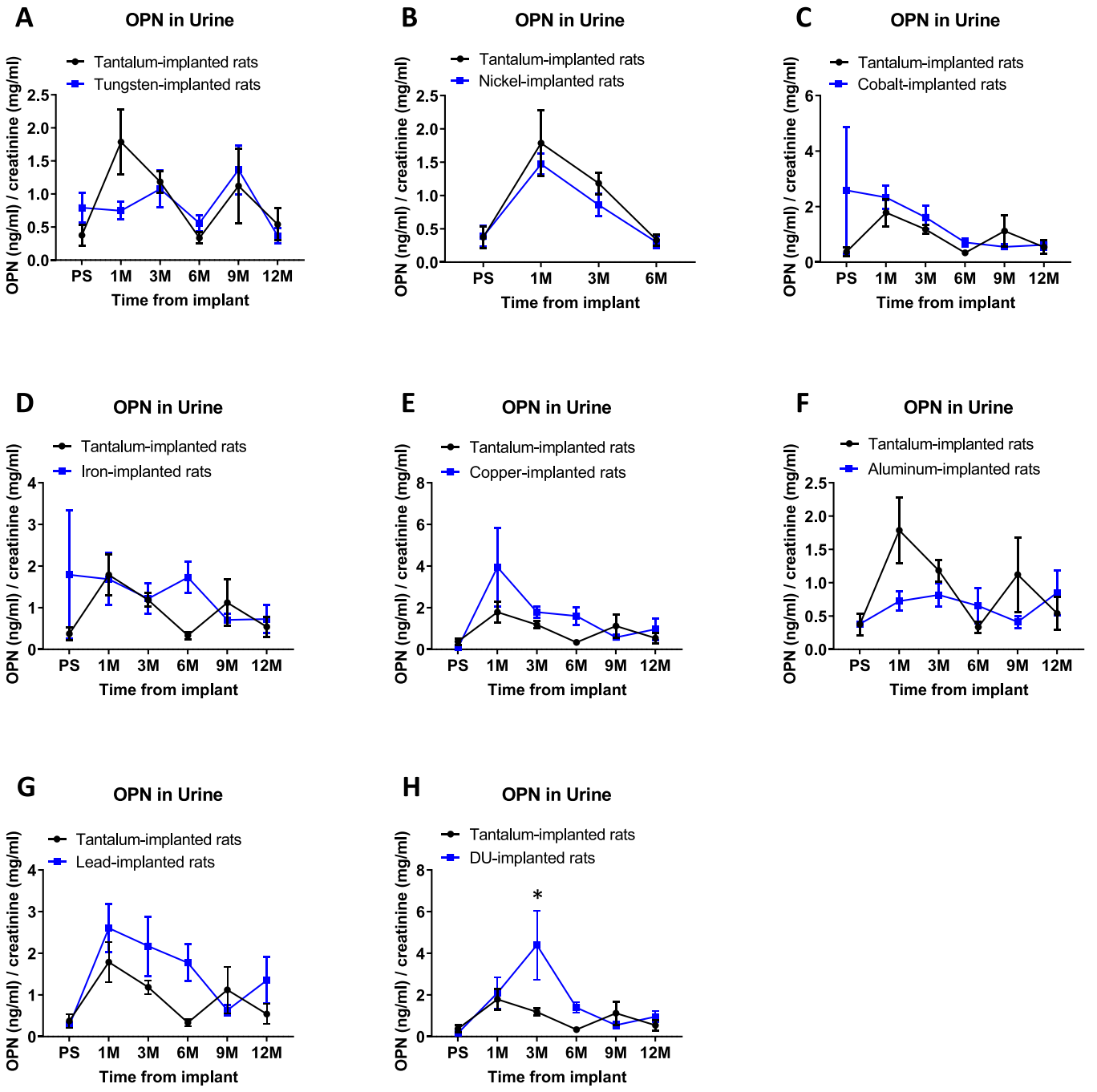

Fig. 8. Urinary OPN levels.
Data presented as OPN normalized to creatinine values in urine collected from multiple time points from individual animals. Each panel compares values in urine from the Ta-implanted animals as controls (black circles/line) vs specific target metal-implanted animals (blue squares/line). Error bars represent standard error of the mean. An * indicates a significant difference between Ta- and target metal-animals at that time point, $p < 0.05$.

4. Discussion

Injuries with embedded metal fragments are an inevitable result of armed conflicts. In some cases, the embedded fragment is the primary injury sustained, while in other instances it might be secondary to a more significant trauma. Regardless, the short- and long-term health effects of embedded metal fragments are an emerging medical concern. Compounding the issue is the fact that there is no limit (other than the periodic table) of what metals might be found in an embedded fragment wound and, for the most part, the toxicological and carcinogenic effects of many metals are not yet known. Previous research on embedded metal fragments suggests that many are capable of solubilizing with the released metal ions being excreted in the urine and, in some cases, sequestering in specific organs of the body [12,14,16,21–23,56]. Because of the recent conflicts in Iraq and Afghanistan, the U.S. Department of Defense and the Department of Veterans' Affairs have developed a list of "metals of concern" with respect to embedded fragment injuries [17,18]. In this study we selected metals from that list and, using a rodent model to study the effects of embedded metals, assessed the associated health effects. We report here the urinary levels of these metals as well as their effects on a battery of renal biomarkers using a within-subjects experimental setup.

For most of the metals tested, significantly elevated levels were measured in the urine starting at 1 M post-implantation with elevated

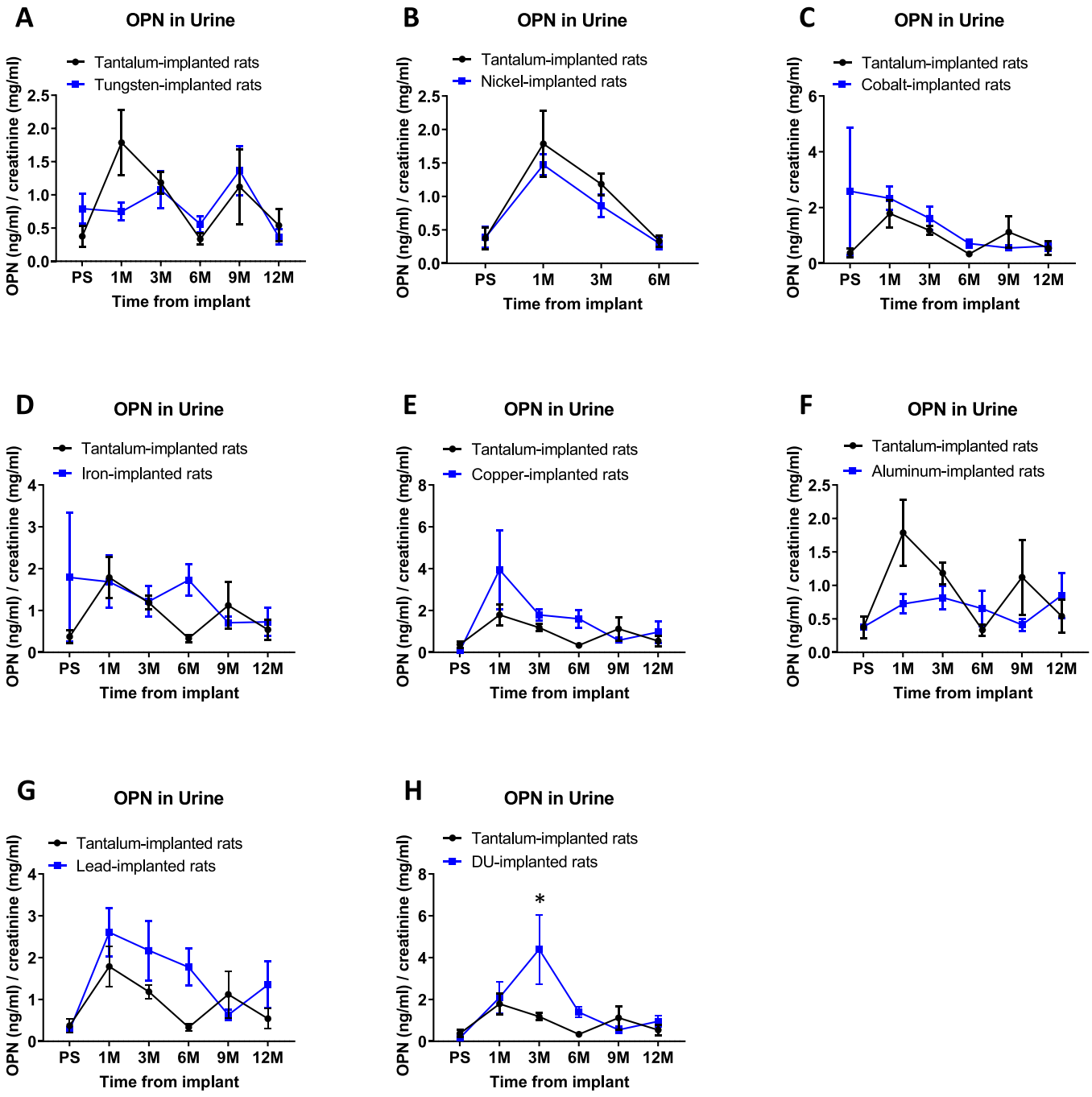

Fig. 9. Urinary KIM-1 in urine.
Data presented as KIM-1 normalized to creatinine values in urine collected from multiple time points from individual animals. Each panel compares values in urine from the Ta-implanted animals as controls (black circles/line) vs specific target metal-implanted animals (blue squares/line). Error bars represent standard error of the mean. An * indicates a significant difference between Ta- and target metal-animals at that time point, $p < 0.05$.

levels continuing for the life of the animal. However, three of the metals tested showed no significant increase in urinary levels. Urinary levels of iron, copper, and aluminum in the metal-implanted rats were not different than that of control animals. It should be noted that there are significant levels of these metals in the tap water used for animal care in our facility [50,51] and excretion of these endogenous metals may have masked any subtle changes in metal excretion due to solubilization of the implanted pellets. It should also be noted that to minimize collection time and thus eliminate any undue stress on the rats, urine collections were limited to a two-hour period with the hydrophobic sand. Basically, this represents a spot collection rather than the historical standard of a 24-h collection in a confined-space metabolic cage. However, we had previously demonstrated no difference in urinary parameters between equal-time collections using hydrophobic sand versus metabolic cage [50–52].

The same spot-collection caveat applies when considering the analysis of the urinary markers of kidney damage. Because of the complex composition (structure/function) of the kidney, it is generally agreed that multiple biomarkers will be required to adequately assess adverse effects induced by a potential toxin [57–59]. Of the urinary biomarkers measured, many were decreased at 1 M post-implantation for practically all the metals tested, except for depleted uranium. Whether this is a result of decreased expression or excretion of the various proteins, an increase in reabsorption in the kidney, or only an artifact of normalizing

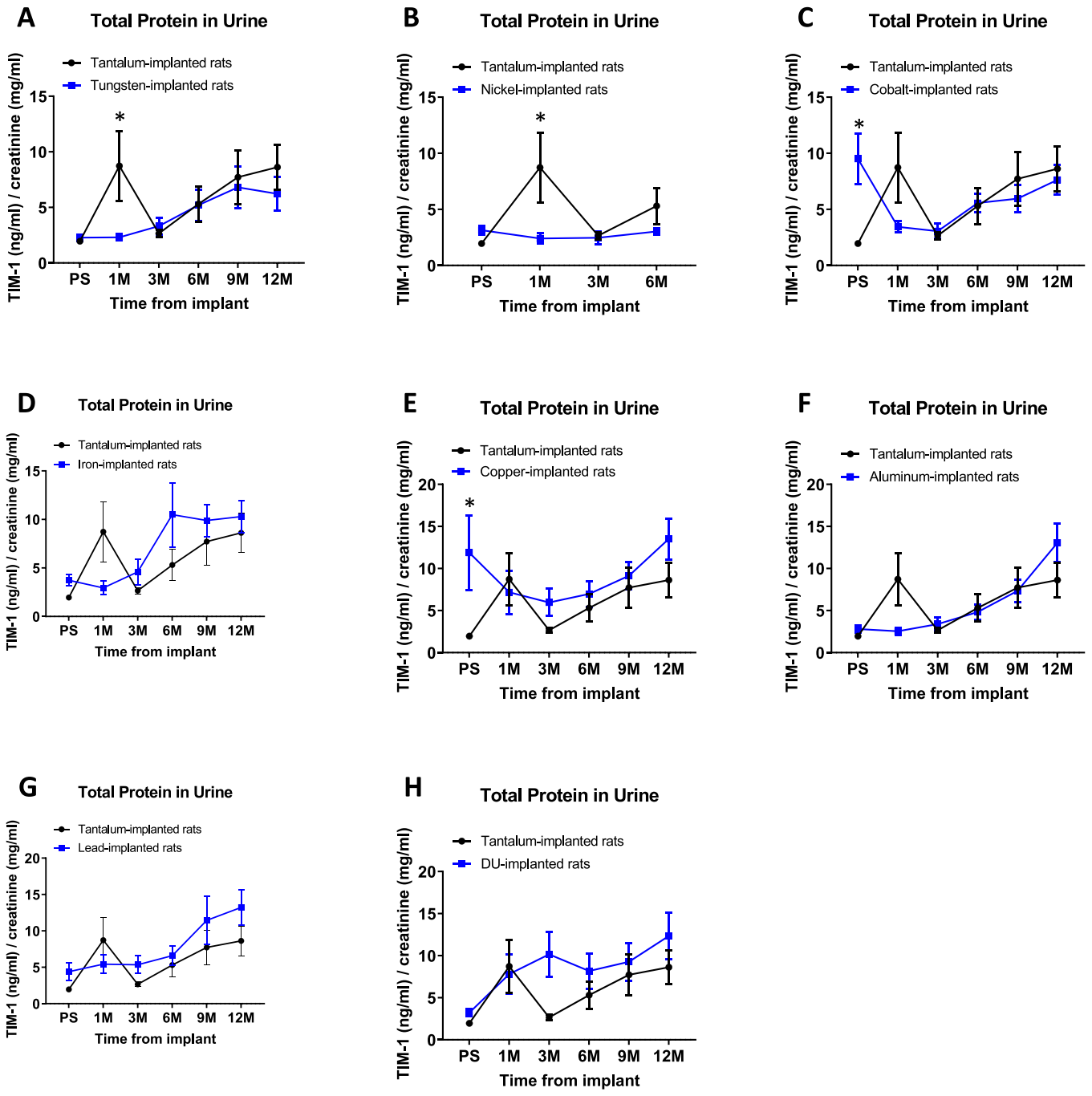

Fig. 10. Total protein levels in urine.
Data presented as total protein normalized to creatinine values in urine collected from multiple time points from individual animals. Each panel compares values in urine from the Ta-implanted animals as controls (black circles/line) vs specific target metal-implanted animals (blue squares/line). Error bars represent standard error of the mean. An * indicates a significant difference between Ta- and target metal-animals at that time point, $p < 0.05$.

to low creatinine expression in the 1 M control (Ta-implanted) animals is not known at this time. After the 1 M time point, all markers assessed return to control values. For the iron group at the 6 M post-implantation point, RBP, NGAL, and KIM-1 were all significantly higher than control indicating potential damage to the proximal tubule region of the kidney even though urinary iron levels were not significantly different. However, this biomarker increase was transient, as values returned to control by 9 M. Similar increases in several proximal tubule markers were seen at 3 and 6 M post-implantation in the DU group. Again, over time these markers returned to control levels. Uranium is a known kidney toxin that damages the proximal tubule area and embedded fragments of DU have been shown to affect several proximal tubule markers [60]. It should be noted however that the amount of DU implanted in those rats far exceeded the amount implanted in this study, indicating that even low amounts of embedded DU, once solubilized, can adversely but transiently affect the kidney. In addition, it has been proposed that the kidney has a substantial capacity to repair its tubular epithelial regions [61] and that repaired epithelium appears more resistant to further uranium-induced damage [62]. It should also be noted that along with being indicators of renal damage, some of the urinary biomarkers also participate in the repair of damage. For example, KIM-1 is a biomarker of both acute and chronic renal injury [63]. However, its

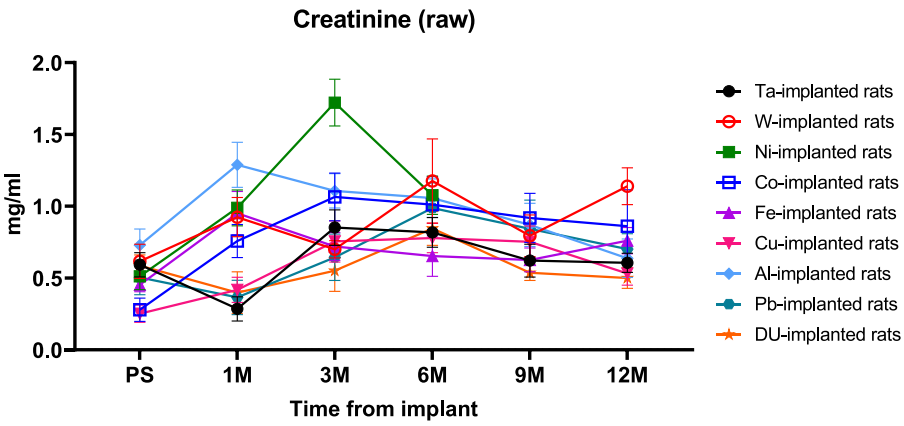

Fig. 11. Urinary creatinine values.
Data presented as creatinine (mg/mL) in urine samples without normalization, since this data is used to normalize metal and other biomarker concentrations. Within subject values are presented as connected lines for a particular metal implant group over urine collection times. Ta – black circle, W – red open circle, Ni – green square, Co – blue open square, Fe – purple triangle, Cu – pink upside down triangle, Al – light blue diamond, Pb – teal hexagon, DU – orange star.

over-expression in proximal renal tubular epithelial cells induces the transformation of these cells into those with phagocytic ability. These cells in conjunction with KIM-1 can identify and eliminate apoptotic bodies resulting from the programmed death of damaged cells [64]. Further, by activation of the ERK/MAPK pathway, over-expression of KIM-1 promotes the proliferation of renal tubular epithelial cells which helps to initiate renal repair [65]. Although there were limited significant differences in urinary levels of KIM-1 as a result of metal implantation, it is not known whether even low levels of KIM-1 could initiate renal repair thus preventing more extensive damage as metal-exposure times increase. This could also explain the return to "normal" values of many of the urinary markers that showed deviations from control at the 1 M post-implantation time point but showed no significant differences at the later time points. Most notably, histopathological examination indicated no overt signs of long-term renal damage. Although well beyond the scope of this study, an investigation into KIM-1 expression changes as a result of metal implantation and its concomitant role in the repair of damaged renal tubular epithelial cells, especially with respect to the signaling pathways involved, would be worthwhile.

During the development and validation of this rodent embedded fragment method an attempt was made to correlate urine uranium levels found in U.S. military personnel wounded with DU fragments with embedded DU pellets in the rat. It was found that from 4 to 20 implanted pellets implanted per rat gave a reasonable correlation with respect to urine uranium levels in wounded individuals [47]. It is not known whether these assumptions would hold for other military-relevant metals. In fact, to minimize potential adverse health effects due to excessive metal loads and based upon our earlier studies, we implanted a limited number of pellets. As such, apart from nickel, there were no metal-associated adverse health issues observed. Most notable was the absence of overt renal effects as determined by histopathological examination of the kidney. Nickel, a known carcinogen, did result in 100 % tumor formation at the metal implantation site [49] resulting in the early euthanasia of this cohort. Cobalt also induced tumors at the implantation site (87 % incidence), as did copper (13 % incidence); however, in neither case were the tumors severe enough to warrant euthanasia under our IACUC protocol [66]. It can be difficult to compare surgically implanted metal pellets in rodents to metal loads in wounds suffered by humans due to the paucity of case reports. However, a recent publication reporting on the metal mobilization from embedded fragments removed from an Iraq War veteran included a thorough description of the physical characteristics, including size, of the surgically excised fragments [21]. Although the wounded individual had many retained fragments, only three were surgically removed because of discomfort. Based on the reported size, we calculated the volume of these fragments which ranged from 0.5 mm^3 to 200 mm^3. The volume of a single pellet (1 mm x 2 mm) used in our study is 1.57 mm^3. Calculating the "human equivalent" of this one pellet gives an estimated volume range of 190 to 366 mm^3 assuming an average rat pre-surgery mass of 300 gm or average pre-euthanasia mass of 580 gm, respectively, as well as the standard "reference man" mass of 70 kg [67]. Therefore, the volume of one rat-implanted pellet is comparable to the volume of a reported excised fragment from a wounded individual.

5. Conclusion

This study demonstrated that pellets of military-relevant metals implanted in the gastrocnemius muscle of rats to simulate a shrapnel wound solubilized over time. With few exceptions, the metals were excreted in the urine of the implanted rats at significantly higher levels than in control animals. While the implanted metals had limited effects on urinary kidney biomarkers, we would expect that increased metal loads would result in much more extensive renal damage based upon our metal excretion results. This study suggests the need for continued surveillance of individuals wounded with metal fragments with urinary metal levels and kidney biomarker assays of particular importance.

Funding

The project described was supported by the grant Health Effects of Blast Injuries and Embedded Metal Fragments (W81XWH-16-2-0058) from the Congressionally Directed Medical Research Program (CDMRP) Peer-reviewed Medical Research Program. All procedures involving animals were (a) conducted with maximal possible well-being of the rats, (b) approved by the AFRRI IACUC prior to the start of the study under protocol 2016−05-006, and (c) performed in compliance with the guidelines set forth in the *Guide for the Care and Use of Laboratory Animals* in an AAALAC-I-accredited facility. The views expressed in the paper are those of the authors and do not reflect the official policy or position of the Armed Forces Radiobiology Research Institute, Uniformed Services University, Department of Defense, or U.S. Government. The use of the LabSand brand of hydrophobic sand in this work does not represent an endorsement of the product or company by the U. S. Government.

CRediT authorship contribution statement

Jessica F. Hoffman: Data curation, Formal analysis, Investigation, Methodology, Software, Validation, Visualization, Writing - review & editing. **Vernieda B. Vergara:** Data curation, Investigation, Methodology, Software, Validation, Writing - review & editing. **Anya X. Fan:** Data curation, Investigation, Methodology, Validation, Visualization, Writing - review & editing. **John F. Kalinich:** Conceptualization, Data curation, Funding acquisition, Investigation, Methodology, Project administration, Resources, Software, Supervision, Validation, Visualization,

A: Tungsten

	1	3	6	9	12
ALB					
ALP					
B2M					
NAG					
RBP					
NGAL					
OPN					
KIM-1					
Protein					

B: Nickel

	1	3	6	9	12
ALB					
ALP					
B2M					
NAG					
RBP					
NGAL					
OPN					
KIM-1					
Protein					

C: Cobalt

	1	3	6	9	12
ALB					
ALP					
B2M					
NAG					
RBP					
NGAL					
OPN					
KIM-1					
Protein					

D: Iron

	1	3	6	9	12
ALB					
ALP					
B2M					
NAG					
RBP					
NGAL					
OPN					
KIM-1					
Protein					

E: Copper

	1	3	6	9	12
ALB					
ALP					
B2M					
NAG					
RBP					
NGAL					
OPN					
KIM-1					
Protein					

F: Aluminum

	1	3	6	9	12
ALB					
ALP					
B2M					
NAG					
RBP					
NGAL					
OPN					
KIM-1					
Protein					

G: Lead

	1	3	6	9	12
ALB					
ALP					
B2M					
NAG					
RBP					
NGAL					
OPN					
KIM-1					
Protein					

H: Depleted Uranium

	1	3	6	9	12
ALB					
ALP					
B2M					
NAG					
RBP					
NGAL					
OPN					
KIM-1					
Protein					

Fig. 12. Comparison of biomarker levels from metal-implanted rats.
"Heat map" depiction of renal biomarkers in urine of metal-implanted rats after 1, 3, 6, 9, and 12 M post-implantation. Blue block indicates a statistically significant result that is lower than control; yellow block indicates no statistical difference between the experimental group and control; red block indicates a statistically significant value that is greater than control value.

Writing - original draft, Writing - review & editing.

Declaration of Competing Interest

The authors declare no conflict of interest. The funders had no role in the design of the study; in the collection, analyses, or interpretation of data; in the writing of the manuscript, or in the decision to publish the results.

Acknowledgements

The authors would like to thank Raisa Marshall and William Danchanko for their expertise in the pellet implantation surgeries, animal welfare checks, and tissue collection. The authors would also like to thank W. Louis Wilkins for histopathology support.

Appendix A. Supplementary data

Supplementary material related to this article can be found, in the online version, at doi:https://doi.org/10.1016/j.toxrep.2021.02.023.

References

[1] M.M. Manring, A. Hawk, J.H. Calhoun, R.C. Andersen, Treatment of war wounds – a historical review, Clin. Ortho. Rel. Res. 467 (8) (2009) 2168–2191, https://doi.org/10.1007/s11999-009-0738-5.

[2] J.F. Kalinich, E.A. Vane, J.A. Centeno, J.M. Gaitens, K.S. Squibb, M.A. McDiarmid, C.E. Kasper, Embedded metal fragments, Ann. Rev Nurs. Res. 32 (2014) 63–78, https://doi.org/10.1891/0739-6686.32.63.

[3] P.J. Dougherty, H.C. Eidt, Wound ballistics: minie ball vs. Full metal jacketed bullets – a comparison of Civil War and Spanish-American War firearms, Mil. Med. 174 (4) (2009) 403–407, https://doi.org/10.7205/MILMED-D-02-2307.

[4] N.L. Schenck, B.S. Kronman, Hoarseness and mass in the neck 30 years after penetrating shrapnel injury, Ann. Otol. Rhinol. Laryngol. 86 (2) (1977) 259, https://doi.org/10.1177/000348947708600220.

[5] J. Knox, A. Wilkinson, Shrapnel presenting with symptoms 62 years after wounding, Brit. Med. J. (Clin. Res. Ed.) 283 (6285) (1981) 193, https://doi.org/10.1136/bmj.283.6285.193.

[6] R.P. Symonds, C. Mackay, P. Morley, The late effect of grenade fragments, J. Royal Army Med. Corps 131 (2) (1985) 68–69.

[7] G. Lindeman, M.J. McKay, K.L. Taubman, A.M. Bilous, Malignant fibrous histiocytoma developing in bone 44 years after shrapnel trauma, Cancer 66 (10) (1990) 2229–2232. DOI: 10.1002/1097-0142(19901115)66:10<2229::AID-CNCR2820661032>3.0.CO;2-X.

[8] D.A. Ligtenstein, J.L.M. Krijnen, B.R.H. Jansen, F. Eulderink, Forgotten injury: a late benign complication of an unremoved shrapnel fragment - case report, J. Trauma-Injury Infect. Crit. Care 36 (4) (1994) 580–582, https://doi.org/10.1097/00005373-199404000-00022.

[9] S. Eylon, R. Mosheiff, M. Liebergall, E. Wolf, L. Brocke, A. Peyser, Delayed reaction to shrapnel retained in soft tissue, Injury: int, J. Care Injured 36 (2) (2005) 275–281, https://doi.org/10.1016/j.imjury.2004.09.005.

[10] IARC Monograph on the Evaluation of Carcinogenic Risk to Humans. Volume 74. Surgical Implants and Other Foreign Bodies, IARC Lyon, France, 1999, pp. 113–229.

[11] M.A. Kane, C.E. Kasper, J.F. Kalinich, Protocol for the assessment of potential health effects from embedded metal fragments, Mil. Med. 174 (3) (2009) 265–269, https://doi.org/10.7205/MILMED-D-02-2808.

[12] T.C. Pellmar, A.F. Fuciarelli, J.W. Ejnik, M. Hamilton, J. Hogan, S. Strocko, C. Emond, H.M. Mottaz, M.R. Landauer, Distribution of uranium in rats implanted with depleted uranium pellets, Toxicol. Sci. 49 (1) (1999) 29–39, https://doi.org/10.1093/toxsci/49.1.29.

[13] F.F. Hahn, R.A. Guilmette, M.D. Hoover, Implanted depleted uranium fragments cause soft tissue sarcomas in the muscles of rats, Environ. Health Persp. 110 (1) (2002) 51–59, https://doi.org/10.1289/ehp.0211051.

[14] J.F. Kalinich, C.A. Emond, T.K. Dalton, S.R. Mog, G.D. Colman, J.E. Kordell, A. C. Miller, D.E. McClain, DE, embedded weapons-grade tungsten alloy shrapnel rapidly induces metastatic high-grade rhabdomyosarcomas in F344 rats, Environ. Health Persp. 113 (6) (2005) 729–734, https://doi.org/10.1289/ehp.7791.

[15] B.E. Schuster, L.E. Roszell, L.E. Murr, D.A. Ramirez, J.D. Demaree, B.R. Klotz, A. B. Rosencrance, W.E. Dennis, W. Bao, E.J. Perkins, J.F. Dillman, D.I. Bannon, In vivo corrosion, tumor outcome, and microarray gene expression for two types of muscle-implanted tungsten alloys, Toxicol. Appl. Pharmacol. 265 (1) (2012) 128–138, https://doi.org/10.1016/j.taap.2012.08.025.

[16] C.A. Emond, V.B. Vergara, E.D. Lombardini, S.R. Mog, J.F. Kalinich, Induction of rhabdomyosarcoma by embedded military-grade tungsten/nickel/cobalt not by tungsten/nickel/iron in the B6C3F1 mouse, Int. J. Toxicol. 34 (1) (2015) 44–54, https://doi.org/10.1177/1091581814565038.

[17] Policy on Analysis of Metal Fragments Removed from Department of Defense Personnel (Policy # : 07-029, Date: 12/18/2007) https://www.health.mil/Military-Health-Topics/Health-Readiness/Environmental-Exposures?page=2#pagingAnchor. [Accessed 03 December 2020].

[18] Screening and Evaluation Protocol for Veterans With Embedded Fragments Who Served in Iraq and/or Afghanistan Post-september 11, 2001 (April 6, 2017) https://www.va.gov/VHAPublications/ViewPublication.asp?pub_ID=5372. [Accessed 03 December 2020].

[19] C.A. Emond, J.F. Kalinich, Biokinetics of embedded surrogate radiological dispersal device material, Health Phys. 102 (2) (2012) 124–136, https://doi.org/10.1097/HP.0b013e31823095e5.

[20] J.A. Centeno, D.A. Rogers, G.B. van der Voet, E. Fornero, L. Zhang, F.G. Mullick, G. D. Chapman, A.O. Olabisi, D.J. Wagner, A. Stojadinovic, B.K. Potter, Embedded fragments – a unique exposure situation and concerns of possible health effects, Int. J. Environ. Res. Pub. Health 11 (2) (2014) 1261–1278, https://doi.org/10.3390/ijerph110201261.

[21] J.M. Gaitens, J.A. Centeno, K.S. Squibb, M. Condon, M.A. McDiarmid, Mobilization of metal from retained embedded fragments in a blast-injured Iraq War Veteran, Mil. Med. 181 (6) (2016) e625–e629, https://doi.org/10.7205/MILMED-D-15-00432.

[22] J.M. Gaitens, M. Condon, K.S. Squibb, J.A. Centeno, M.A. McDiarmid, Metal exposure in veterans with embedded fragments from war-related injuries: early findings from surveillance efforts, J. Occ. Environ. Med. 59 (11) (2017) 1056–1062, https://doi.org/10.1097/JOM.0000000000001119.

[23] M.A. McDiarmid, J.M. Gaitens, S. Hines, M. Condon, T. Roth, M. Oliver, P. Gucer, L. Brown, J.A. Centeno, M. Dux, K.S. Squibb, The US Department of Veterans' Affairs depleted uranium cohort at 25 years: longitudinal surveillance results, Environ. Res. 152 (2017) 175–184, https://doi.org/10.1016/j.envres.2016.10.016.

[24] J. Daniel, H. Ziaee, C. Pradhan, P.B. Pynsent, D.J.W. McMinn, Renal clearance of cobalt in relation to the use of metal-on-metal bearings in hip arthroplasty, J. Bone Joint Surg. 92A (4) (2010) 840–845, https://doi.org/10.2106/JBJS.H.01821.

[25] A. Sarmiento-Gonzalez, J.R. Encinar, J.M. Marchante-Gayon, A. Sanz-Medel, Titanium levels in the organs and blood of rats with a titanium implant, in the absence of wear, as determined by double-focusing ICP-MS, Analyt. Bioanalyt. Chem. 393 (2009) 335–343, https://doi.org/10.1007/s00216-008-2449-2.

[26] J.-J. Aguilera-Correa, A. Aunon, M. Boiza-Sanchez, I. Mahillo-Fernandez, A. Mediero, D. Equibar-Blazquez, A. Conde, M.-A. Arenas, J.-J. de-Damborenea, J. Cordero-Ampuero, J. Esteban, Urine aluminum concentration as a possible implant biomarker of *Pseudomonas aeruginosa* infection using a fluorine- and phosphorus-doped Ti-6Al-4V alloy with osseointegration capacity, ACS Omega 4 (2019) 11815–11823, https://doi.org/10.1021/acsomega.9b00898.

[27] S.T. Mahieu, M. Gionotti, N. Millen, M.M. Elias, Effect of chronic aluminum on renal function, cortical renal oxidative stress and cortical renal organic anion transport in rats, Arch. Toxicol. 77 (11) (2003) 605–612, https://doi.org/10.1007/s00204-003-0496-1.

[28] J.Y. Liu, Q. Wang, X.D. Sun, X. Yang, C.C. Zhuang, F.B. Xu, Z. Cao, Y.F. Li, The toxicity of aluminum chloride on kidney of rats, Biol. Trace Elem. Res. 173 (3) (2016) 339–344, https://doi.org/10.1007/s12011-016-0648-9.

[29] R. Tyagi, P. Rana, M. Guptra, A.R. Khan, D. Bhatnagar, P.J.S. Bhalla, S. Chaturvedi, R.P. Tripathi, S. Khushu, Differential biochemical response of rat kidney towards low and high doses of NiCl2 as revealed by NMR spectroscopy, J. Appl. Toxicol. 33 (2) (2013) 134–141, https://doi.org/10.1002/jat.1730.

[30] R. Zhou, Y. Xu, J. Shen, L. Han, X. Chen, X. Feng, X. Kuang, Urinary KIM-1: a novel biomarker for evaluation of occupational exposure to lead, Sci. Reports 6 (2016) 38930, https://doi.org/10.1038/srep38930.

[31] R.B. Jain, Lead and kidney: concentrations, variabilities, and associations across the various stages of glomerular function, J. Trace Elem. Med. Biol. 54 (2019) 36–43, https://doi.org/10.1016/j.temb.2019.03.007.

[32] P. Kurttio, A. Harmoinen, H. Saha, L. Salonen, Z. Karpas, H. Komulainen, A. Auvinen, Kidney toxicity of ingested uranium from drinking water, Am. J. Kidney Dis. 47 (6) (2006) 972–982, https://doi.org/10.1053/j.ajkd.2006.03.002.

[33] J.A. Bijlsma, P. Slottje, A.C. Huizink, J.W.R. Twisk, G.B. van der Voet, F.A. de Wolff, F. Vanhaecke, L. Moens, T. Smid, Urinary uranium and kidney function parameters in professional assistance workers in the Epidemiological Study Air Disaster in Amsterdam (ESADA), Nephrol. Dial. Transplant. 23 (1) (2008) 249–255, https://doi.org/10.1093/ndt/gfm461.

[34] A. Weiss, L. Spektor, L.A. Cohen, L. Lifshitz, I.M. Gold, D.L. Zhang, M. Truman-Rosentsvit, Y. Leichtmann-Bardoogo, A. Nyska, S. Addadi, T.A. Rouault, E. G. Meyron-Holtz, Orchestrated regulation of iron trafficking proteins in the kidney during iron overload facilitates iron retention, PLoS One 13 (10) (2018), e0204471, https://doi.org/10.1371/journal.pone.0204471.

[35] J. Biernawska, J. Bober, K. Kotfis, I. Nocen, A. Bogacka, E. Barnik, D. Chlubek, M. Zukowski, Iron excretion in patients with acute kidney injury after cardiac surgery, Adv. Clin. Exp. Med. 27 (12) (2018) 1671–1676, https://doi.org/10.17219/acem/75504.

[36] S.E.G. van Raaij, A.J. Rennings, B.J. Biemond, S.E.M. Schols, E.T.G. Wiegerinck, H. M.J. Roelofs, E.J. Hoorn, S.B. Walsh, T. Nijenhuis, D.W. Swinkels, R.P.L. van Swelm, Iron handling by the human kidney: glomerular filtration and tubular reabsorption both contribute to iron excretion, Amer. J. Physiol. – Renal Physiol. 316 (3) (2019) F606–F614, https://doi.org/10.1152/ajprenal.00425.2018.

[37] R. Flores-Ramirez, E. Rico-Escobar, J.E. Nunez-Monreal, E. Garcia-Noeto, L. Carrizales, C. Ilizaliturri-Hernandez, F. Diaz-Barriga, Children exposure to lead in contaminated sites, Salud Publica Mex. 54 (4) (2012) 383–392.

[38] M. Cardenas-Gonzalez, C. Osorio-Yanez, O. Gaspar-Ramirez, M. Paykovic, A. Ochoa-Martinez, D. Lopez-Ventura, M. Medeiros, O.C. Barbier, I.N. Perez-Maldonado, V.S. Sabbisetti, J.V. Bonventre, V.S. Vaidya, Environmental exposure to arsenic and chromium in children is associated with kidney injury molecule-1, Environ. Res. 150 (2016) 653–662, https://doi.org/10.1016/j.envres.2016.06.032.

[39] X.F. Cui, H.G. Cheng, X.L. Liu, E. Giubilato, A. Critto, H.X. Sun, L. Zhang, Cadmium exposure and early renal effects in the children and adults living in a tungsten-molybdenum mining area of South China, Environ. Sci. Pollut. Res. 25 (15) (2018) 15089–15101, https://doi.org/10.1007/s11356-018-1631-0.

[40] M. Valcke, N. Ouellet, M. Dube, E.A.L. Sidi, A. LeBlanc, L. Normandin, C. Balion, P. Ayotte, Biomarkers of cadmium, lead and mercury exposure in relation with early biomarkers of renal dysfunction and diabetes: results from a pilot study among aging Canadians, Toxicol. Lett. 312 (2019) 148–156, https://doi.org/10.1016/j.toxlet.2019.05.014.

[41] L. Diaz de Leon-Martinez, M. Ortega-Romero, J.M. Grimaldo-Galeana, O. Barbier, K. Vargas-Berrones, M.E. Garcia-Arreola, M. Rodriguez-Aguilar, R. Flores-Ramirez, Assessment of kidney health and exposure to mixture pollutants in the Mexican indigenous population, Environ Sci. Pollut. Res. 27 (2020) 34557–34566. DOI: 101007/s11356-020-09619-x.

[42] A. Kataria, L. Trasande, H. Trachtman, The effects of environmental chemicals on renal function, Nat. Rev. Nephrol. 11 (2015) 610–625, https://doi.org/10.1038/nrneph.2015.94.

[43] M.I. Jimenez-Cordova, M. Cardenas-Gonzalez, G. Aguilar-Madrid, L.C. Sanchez-Pena, A. Barrera-Hernandez, I.A. Dominguez-Guerrero, C. Gonzalez-Horta, O. C. Barbier, L.M. Del Razo, Evaluation of kidney injury biomarkers in an adult Mexican population environmentally exposed to fluoride and low arsenic levels, Toxicol. Appl. Pharmacol. 352 (2018) 97–106, https://doi.org/10.1016/j.taap.2018.05.027.

[44] L. Diaz de Leon-Martinez, F. Diaz-Barriga, O. Barbier, D.L.G. Ortiz, M. Ortega-Romero, F. Perez-Vazquez, R. Flores-Ramirez, Evaluation of emerging biomarkers

of renal damage and exposure to aflatoxin-B_1 in Mexican indigenous women: a pilot study, Environ Sci. Pollut. Res. 26 (2019), https://doi.org/10.1007/s11356-019-04634-z, 12295-12216.
[45] N. Perez-Herra, L. Diaz de Leon-Martinez, R. Flores-Ramirez, O. Barbier, M. Ortega-Romero, F. May-Euan, K. Saldana-Villanueva, J. Perera-Rios, F.J. Perez-Vazquez, Evaluation of benzene exposure and early biomarkers of kidney damage in children exposed to solvents due to precarious work in Ticul, Yucatan, Mexico, Ann. Global Health 85 (1) (2019) 94, https://doi.org/10.5334/aogh.2482.
[46] National Research Council, Guide for the Care and Use of Laboratory Animals, eighth edition, The National Academies Press, Washington, DC, 2011. DOI.org/10.17226/12910.
[47] C.A. Castro, K.A. Benson, V. Bogo, E.G. Daxon, J.B. Hogan, H.M. Jacocks, M. R. Landauer, S.A. McBride, C.W. Shehata, Establishment of an Animal Model to Evaluate the Biological Effects of Intramuscularly Embedded Depleted Uranium Fragments, Armed Forces Radiobiology Research Institute, Bethesda, MD, 1996. Technical Report 96-3.
[48] N. Percie du Sert, V. Hurst, A. Ahluwalia, S. Alam, M.T. Avey, M. Baker, W. J. Browne, A. Clark, I.C. Cuthill, U. Dirnagi, M. Emerson, P. Garner, S.T. Holgate, D.W. Howells, N.A. Karp, S.E. Lazic, K. Lidster, C.J. MacCallum, M. Macleod, E. J. Pearl, O.H. Petersen, F. Rawle, P. Reynolds, K. Rooney, E.S. Sena, S. D. Silberberg, T. Steckler, H. Wurbel, The ARRIVE guidelines 2.0: updated guidelines for reporting animal research, PLoS Biol. 18 (7) (2020), e3000410, https://doi.org/10.1371/journal.pbio.3000410.
[49] J.F. Hoffman, V.B. Vergara, J.F. Kalinich, Brain region- and metal-specific effects of embedded metals in a shrapnel wound model in the rat, NeuroToxicology 83 (2021) 116–128, https://doi.org/10.1016/j.neuro.2021.01.001.
[50] J.F. Hoffman, V.B. Vergara, S.R. Mog, J.F. Kalinich, Hydrophobic sand is a non-toxic method of urine collection, appropriate for urinary metal analysis in the rat, Toxics 5 (4) (2017) 25, https://doi.org/10.3390/toxics5040025.
[51] J.F. Hoffman, A.X. Fan, E.H. Neuendorf, V.B. Vergara, J.F. Kalinich, Hydrophobic sand versus metabolic cages: a comparison of urine collection methods for rats (*Rattus norvegicus*), J. Am. Assoc. Lab. Anim. Sci. 57 (1) (2018) 51–57.
[52] J.F. Hoffman, I.J. Vechetti, A.P. Alimov, J.F. Kalinich, J.J. McCarthy, C. A. Peterson, Hydrophobic sand is a viable method of urine collection from the rat for extracellular vesicle biomarker analysis, Molec. Genet. Metab. Rpt. 21 (2019), 100505, https://doi.org/10.1016/j.ymgmr.2019.100505.
[53] AVMA Guidelines for the Euthanasia of Animals (2020). https://www.avma.org/sites/default/files/2020-01/2020-Euthanasia-Final-1-17-20.pdf (accessed 18 November 2020).
[54] C. Slot, Plasma creatinine determination. A new and specific Jaffe reaction method, Scand, J. Clin. Lab. Invest. 17 (4) (1965) 381–387, https://doi.org/10.3109/00365516509077065.
[55] D. Heinegard, G. Tiderstrom, Determination of serum creatinine by a direct colorimetric method, Clin. Chim. Acta 43 (1973) 305–310.
[56] J.F. Kalinich, V.B. Vergara, C.A. Emond, Urinary and serum metal levels as indicators of embedded tungsten alloy fragments, Mil. Med. 173 (8) (2008) 754–758, https://doi.org/10.7205/MILMED.173.8.754.
[57] V.S. Vaidya, M.A. Ferguson, J.V. Bonventre, Biomarkers of acute kidney injury, Ann. Rev. Pharmacol. Toxicol. 48 (2008) 463–493, https://doi.org/10.1146/annurev.pharmtox.48.113006.094615.
[58] J.V. Bonventre, V.S. Vaidya, R. Schmouder, P. Feig, F. Dieterle, Next-generation biomarkers for detecting kidney toxicity, Nature Biotechnol. 28 (5) (2010) 436–440, https://doi.org/10.1038/nbt0510-436.
[59] S. Lopez-Giacoman, M. Madero, Biomarkers in chronic kidney disease, from kidney function to kidney damage, World J. Nephrol. 4 (1) (2015) 57–73, https://doi.org/10.5527/wjn.v4.i1.57.
[60] G.Y. Zhu, X.Q. Xiang, X. Chen, L.H. Wang, H.P. Hu, S.F. Weng, Renal dysfunction induced by long-term exposure to depleted uranium in rats, Arch. Toxicol. 83 (1) (2009) 37–46, https://doi.org/10.1007/s00204-008-0326-6.
[61] D.F. Sun, Y. Fujigaki, T. Fujimoto, T. Goto, K. Yonemura, A. Hishida, Relation of distal nephron changes to proximal tubular damage in uranyl acetate-induced acute renal failure in rats, Am. J. Nephrol. 22 (5-6) (2002) 405–416, https://doi.org/10.1159/000065265.
[62] H.C. Hodge, J.N. Stannard, J.B. Hursh, Uranium, plutonium, transplutonic elements, in: 1st ed., in: H.C. Hodge, J.N. Stannard, J.B. Hursh (Eds.), Handbook of Experimental Pharmacology, Vol. 36, Springer-Verlag, New York, 1973, pp. 165–195.
[63] J.Y. Song, J. Yu, G.W. Prayogo, W.D. Cao, Y.M. Wu, Z.J. Jia, A.H. Zhang, Understanding kidney injury molecule 1: a novel immune factor in kidney pathophysiology, Am. J. Transl. Res. 11 (3) (2019) 1219–1229.
[64] T. Ichimura, E.J.P.V. Asseldonk, B.D. Humphreys, L. Gunaratnam, J.S. Duffield, J. V. Bonventre, Kidney injury molecule-1 is a phosphatidylserine receptor that confers a phagocytic phenotype on epithelial cells, J. Clin. Inv. 118 (5) (2008) 1657–1668, https://doi.org/10.1172/JCI34487.
[65] Z.W. Zhang, C.X. Cai, Kidney injury molecule-1 (KIM-1) mediates renal epithelial cell repair via ERK MAPK signaling pathway Mol, Cell. Biochem. 416 (1-2) (2016) 109–116, https://doi.org/10.1007/s11010-016-2700-7.
[66] Y. Wen, I.J. Vechetti, J.F. Hoffman, V.B. Vergara, J.F. Kalinich, J.J. McCarthy, C. A. Peterson, Time-course analysis of the effect of embedded metal on skeletal muscle gene expression, Physiol. Genomics 52 (2020) 575–587, https://doi.org/10.1152/physiolgenomics.00096.2020.
[67] International Commission on Radiological Protection, Report of the Task Group on Reference Man, ICRP Publication 23, Pergamon Press, Oxford, 1975.